UNIVERSITÉ DE LILLE

FACULTÉ DE MÉDECINE HENRI WAREMBOURG

Année : 2022

THÈSE POUR LE DIPLÔME D'ÉTAT

DE DOCTEUR EN MÉDECINE

Les modifications transcriptomiques corrélées à l'augmentation du pourcentage de Gleason 4 dans une cohorte de diagnostic du cancer de la prostate

Présentée et soutenue publiquement le 19 septembre 2022 à 18h00
au Pôle Formation

par Kelly CHEN

JURY

Président :

Monsieur le Professeur Arnauld VILLERS

Assesseurs :

Monsieur le Professeur Xavier LEROY

Madame le Docteur Martine DUTERQUE-COQUILLAUD

Directeur de thèse :

Monsieur le Docteur Jonathan OLIVIER

TABLE DES MATIERES

ABREVIATIONS

%G4	pourcentage de grade de Gleason 4
ADN or DNA	acide désoxyribonucléique
DCE	image dynamique à contraste amélioré
DWI	image pondérée en diffusion
FDR	taux de fausse découverte
FFPE	fixés au formol et inclus dans la paraffine
G4	grade de Gleason 4
H&E	hématoxyline et éosine
IQR	écart interquartile
IRMmp ou mpMRI	imagerie par résonance magnétique multiparamétrique
ISUP	International Society of Urological Pathology
MCCL	longueur maximale de cancer sur carotte de biopsie
ORA	analyse de sur-représentation
PSA	antigène prostatique spécifique
QC	contrôle de qualité
ARN ou RNA	acide ribonucléique
T2W	image pondérée en T2
UCLH	University College London Hospitals

LISTE DES TABLEAUX ET FIGURES

Figure 7: Barplots representing over represented gene sets by genes identified to be correlated to normalised %G4 by differential analysis (%G4 significant genes), in Hallmark (A) and Reactome (B) databases. The universe was the entire database.

Supplementary materials

Table S1: Criteria common to the following prostate cancer risk stratification systems: D'Amico/Association Francaise d'Urologie (2020), European Association of Urology (2021), National Institute for Health and Care Excellence or NICE (2019).

Figure S1: Example of sample processing by HTG.

Figure S2: Principal component analysis (PCA) on the 64 targeted areas with good quality RNA for this study, from 51 different patients.

Figure S3: Model for normalisation of %G4 based on gladular and stroma tissu cell proportion.

Figure S4: Settings for the Pixel classifier and example of trained pixel classifier on H&E images.

Figure S5: Barplots representing over represented gene sets by genes identified to be correlated to normalised %G4 by differential analysis and Pearson's correlation test (%G4 significant genes, only SPINK1 was not found in the database), in Reactome database.

1. INTRODUCTION

Le score de Gleason est un score histologique de classification des motifs et architectures histologiques du cancer de prostate, classés selon leur valeur pronostique, créé au cours du XXe siècle [1]. De nombreuses études ont confirmé la valeur pronostique du score de Gleason [2,3]. Le développement du dépistage du cancer de la prostate et l'utilisation de l'immuno-histo-chimie ont conduit à la conférence ISUP en 2005 qui a révisé les recommandations pour le classement et le score de Gleason [4,5] (**Figure A**).

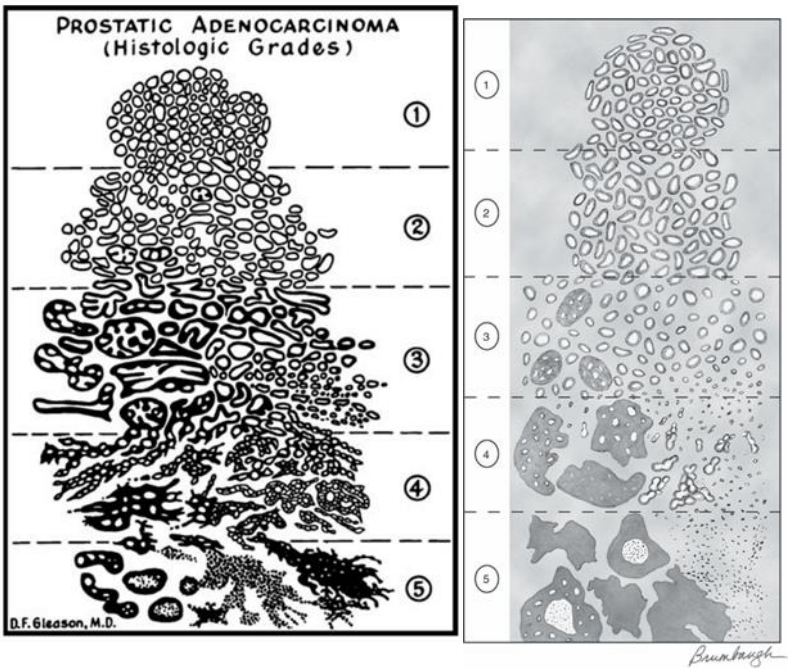

Figure A: Dessin par Gleason de son système de classement standardisé pour l'adénocarcinome de la prostate (à gauche) et illustration de la classification ISUP de 2005 (à droite).

Le score de Gleason modifié de la conférence ISUP 2005 a conduit au changement de répartition des groupes pronostiques, avec moins de score de Gleason 6 et plus de score de Gleason 7 [6]. Dans le groupe hétérogène du score de Gleason 7, le score révisé a trouvé plus de 3+4 et plus de 4+3. Elle a également permis une meilleure discrimination entre les groupes pronostiques [7]. Dans la poursuite d'une médecine plus personnalisée, la question se pose autour de l'importance du grade de Gleason 4, historiquement catégorisé comme un critère binomial (inférieur ou supérieur à 50%). Les systèmes de stratification de risque européen (European Association of Urology, 2021) [8], britannique (National Institute for Health and

Care Excellence ou NICE, 2019) [9], et français (D'Amico/Association Française d'Urologie, 2020) [10] actuels n'intègrent pas le %G4 en tant que variable continue (**Tableau S1**). Une recommandation majeure de la conférence de consensus ISUP de 2014 était de rapporter le pourcentage de grade de Gleason 4 (%G4) pour un score de Gleason de 7 dans les biopsies à l'aiguille et les échantillons de prostatectomie radicale [11]. La classification OMS 2016 des tumeurs de l'appareil urinaire et des organes génitaux masculins recommande également de déclarer le %G4 pour l'adénocarcinome de score de Gleason 7 [12], d'autant plus que cela peut avoir des implications pour les stratégies de prise en charge chez certains patients atteints de grade de Gleason 3+4=7 avec un faible %G4, chez qui il serait possible d'envisager une surveillance active [13].

Ces dernières années, plusieurs études ont trouvé une relation entre le %G4 et le pronostic des patients atteints d'un cancer de la prostate subissant une prostatectomie radicale [14,15]. C'est un facteur prédictif de maladie clinique avancée [16,17], de récidive biochimique [15,18–20], de récidive métastatique [21] et de survie spécifique au cancer [22] . Les taux de récidive biochimique après prostatectomie radicale chez les patients avec biopsie score de Gleason 3+4=7 avec $\leqslant$ 5% cancer de type 4 étaient comparables à ceux de la biopsie score de Gleason 3+3=6 cancer [15,20,23]. Sauter et al [15] ont montré une augmentation continue du risque de récidive biochimique avec un pourcentage croissant de Gleason 4, avec une différence pronostique distincte ($p < 0,0001$) pour Gleason 3 + 4 = 7 faible (1–24 % Gleason 4) vs élevé (25–49 % Gleason 4) et une différence petite entre 40 % G4 et 60 % G4, remettant en question les groupes pronostiques établis. Les modèles multivariables incorporant %G4 dans la prédiction de la récidive biochimique ou de la récidive métastatique se sont révélés précis avec un seuil de 20 % ou 30 % de G4 [21].

Le phénotype et les fonctions des cellules dérivent de la combinaison de gènes activés. En étudiant l'ARN transcrit à partir de ces gènes, nous pouvons savoir quels gènes sont actifs dans un type cellulaire particulier, à un moment particulier. Il indique également quelle protéine pourrait être exprimée ou surexprimée [24]. Les études transcriptomiques intégrées sont une méthode courante pour identifier les voies [25–27] menant à une cible diagnostique ou thérapeutique potentielle, tout en gérant efficacement les ressources et le temps. Les signatures d'expression des gènes ont été étudiées et validées pour prédire le pronostic du cancer de la prostate [28]. Trois sont actuellement disponibles dans le commerce et sont de plus en plus intégrées dans les essais cliniques [29,30]. Decipher (GenomeDx Biosciences,

San Diego, CA, USA), OncotypeDx (Genomic Health, Redwood City, CA, USA) et Prolaris (Myriad Genetics, Salt Lake City, UT, USA) sont des biomarqueurs de stratification des risques qui incluent des données cliniques du patient. Le profilage de l'expression génique a également été étudié pour différencier le modèle de Gleason 3 du 4 [31,32]. Cependant, à ce jour, personne n'a étudié les gènes impliqués avec le %G4 en tant que variable continue.

Compte tenu de l'importance croissante de %G4 dans la sélection des patients, cette étude visait à consolider la compréhension actuelle des voies transcriptomiques sous-jacentes à l'expansion du grade de Gleason 4, en l'examinant d'une nouvelle manière. L'objectif principal de cette étude était d'identifier les gènes différentiellement exprimés entre un %G4 faible et un %G4 élevé, ainsi que d'identifier ceux corrélés avec le %G4 comme une variable continue, dans une cohorte bien définie et de haute qualité d'ARN provenant de biopsies diagnostiques à l'aiguille de la prostate.

2. ARTICLE (anglais)

Transcriptomic changes correlated with increased percentage of Gleason pattern 4 in a cohort of men with diagnostic of prostate cancer.

Keywords:
Biomarkers, Prostatic Neoplasms, Diagnosis, Magnetic Resonance Imaging, Cancer, Prostate, Gleason4, Percent Gleason 4, RNA, Genes,

Abstract

Objective:
It is now recommended to report percentage of Gleason pattern 4 (%G4) with Gleason score 7 prostate adenocarcinoma, rather than the binary 3+4 or 4+3 gradings. The main objective of this study was to identify genes whose expression varies with %G4 and the underlying pathways involved in the emergence of Gleason 4 pattern.

Methods:
Patients were selected from the INNOVATE study, a well described UK, single centre cohort of men with diagnostic of prostate cancer by MRI-targeted biopsy. 51 MRI targeted core needle biopsies containing Gleason 3 and/or 4 without Gleason pattern 5 were included, and tumour areas were macrodissected for molecular analysis. Gene expression data of 2549 cancer-associated genes were generated with the HTG EdgeSeq system coupled with the Illumina Next Generation Sequencing platform. Differential expression analysis was performed on the ends of the cohort, between low %G4 and high %G4. Differentially

expressed genes were further investigated on more samples in an analysis correlating their expression with the %G4 kept as a continuous variable. An enrichment analysis looked for Hallmark and Reactome gene sets which were over-represented in the list of differentially expressed genes.

Results:

We identified a panel of 15 genes of interest by selecting those differentially expressed between low %G4 (0-10%) and high %G4 (40-100%), with an adjusted p-value < 0.05. 12 genes were up-regulated (SPINK1, COMP, ADAMTS1, EFNB2, ISG15, CENPN, IRS2, JAG1, F2R, HEYL, EGR1 and ENG), while 3 genes were down-regulated (CXCL13, BMP5 and ADRA1D). When this panel was tested for its linear correlation with normalised %G4 (adjusted for the proportion of epithelial cells in the sample), 5 of them were significantly correlated to %G4 with a Pearson's correlation coefficient between 0.41 and 0.56 (adjusted p-value < 0.05). The most relevant pathways included androgen signaling, signal transduction, immune response (NOTCH, interferon, TNFα), and cellular responses to stimuli.

Conclusion:

This pilot study was able to find transcriptomic changes correlated with increased %G4. The identified pathways were relevant with existing literature and cancer aggressivity, supporting the growing interest in the interpretation of %G4 as a continuous variable rather than the binary grouping of Gleason score 7 disease into 3+4 and 4+3 for the evaluation of prostate cancer aggressivity. The further study of pathways associated with %G4 could lead to personalised targeted therapy and improve prognosis of a subgroup of Gleason score 7 prostate cancers, a rather heterogeneous risk group.

2.1. Introduction

The modified Gleason score from the 2005 ISUP conference lead to the change of distribution of prognostic groups, with less Gleason score 6 and more Gleason score 7 [6]. In the heterogeneous Gleason score 7 group, the revised scoring found more 3+4 and more 4+3. It also enabled a better discrimination between prognosis groups [7]. In the pursuit of a more personalised medicine, the question arises around the importance of Gleason pattern 4, which was historically categorised as a binomial criteria (below or over 50%). The current European (European Association of Urology, 2021) [8], British (National Institute for Health and Care Excellence ou NICE, 2019) [9], and French (D'Amico/Association Francaise d'Urologie, 2020) [10] risk stratification systems do not incorporate %G4 as a continuous variable (**Table S1**). A major recommendation from the 2014 ISUP Consensus Conference was to report percentage of Gleason pattern 4 (%G4) with Gleason score 7 in both needle biopsies and radical prostatectomy specimens [11]. The 2016 WHO Classification of Tumours of the Urinary System and Male Genital Organs also recommends reporting of %G4 for Gleason score 7 adenocarcinoma [12], especially as it may have implications for management strategies with some patients with Gleason grade 3+4=7 with a low %G4 being considered for active surveillance [13].

In recent years, several studies have found a relationship between %G4 and the prognosis of prostate cancer patients undergoing radical prostatectomy [14,15]. It is a predictor of advanced clinical disease [16,17], biochemical recurrence [15,18–20], metastatic recurrence [21] and cancer-specific survival [22]. The rates of biochemical recurrence following radical prostatectomy in patients with biopsy Gleason score 3+4=7 with ≤ 5% pattern 4 cancer were comparable with those of biopsy Gleason score 3+3=6 cancer [15,20,23]. Sauter et al [15] showed a continuous increase of biochemichal recurrence risk with increasing percentage of Gleason 4, with a distinct prognostic difference ($p < 0.0001$) for Gleason 3 + 4 = 7 low (1–24% Gleason 4) vs high (25–49% Gleason 4) and small difference between 40%G4 and 60%G4, questioning established prognostic groups. Multivariable models incorporating %G4 in prediction of biochemical recurrence or metastatic recurrence were shown to be accurate with a threshold of 20% or 30%G4 [21].

Cells phenotype and functions derive from the combination of activated genes. By studying the RNA transcribed from these genes, we can find out which genes are active in a particular cell type, at a particular moment. It also hints at which protein could be expressed or over-expressed [24]. Integrated transcriptomic studies are a common method to identify pathways [25–27] leading to potential diagnostic or therapeutic target, while efficiently managing resources and time. Genes expression signatures have been studied and validated to predict prostate cancer prognosis [28], with three of them currently commercially available and being increasingly incorporated into clinical trials [29,30]. Decipher (GenomeDx Biosciences, San Diego, CA, USA), OncotypeDx (Genomic Health, Redwood City, CA, USA) and Prolaris (Myriad Genetics, Salt Lake City, UT, USA) are risk stratification biomarkers which include clinical data from the patient. Gene expression profiling has also been studied to differentiate Gleason pattern 3 from 4 [31,32]. However, to date, no one has studied the genes involved with %G4 as a continuous variable.

Given the growing importance of %G4 in patient triage, this study aims to help consolidate the current understanding of the transcriptomic pathways underlying the expansion of Gleason pattern 4, by looking at in in a novel way. The main objective of this study was to identify genes differentially expressed between low and high %G4 and identify those correlated with %G4 as a continuous variable, in a well-defined and high quality cohort of RNA taken from diagnostic prostate needle biopsies.

2.2. Material and Methods

2.2.1. Patient Population

Patients were selected from the INNOVATE cohort. The INNOVATE study protocol has been described in-depth previously [33]. In brief, men (which inclusion and exclusion criteria are described in **Table 1**) referred with suspected prostate cancer from April 2016 to September 2019 underwent serum and urine collection, pre-biopsy diagnostic mpMRI, followed by MRI-targeted biopsy when indicated as part of usual clinical care. All men underwent a clinical prostate mpMRI at University College London Hospital (UCLH) on either a 1.5T or 3.0 Tesla scanner (Achieva; Philips, Best, the Netherlands / Ingenia, Phillips, Best, the Netherlands / Avanto, Siemens, Erlangen, Germany) using a pelvic-phased array coil. mpMRI sequences included T1-weighted (T1W), T2W, DCE with gadolinium, DWI and apparent diffusion coefficient (ADC) maps. All mpMRIs were scored at UCLH as part of standard clinical practice by experienced uroradiologists using Likert scale for the likelihood of clinically significant prostate [9,34,35], as described previously. Each suspicious area was scored separately. From the 365 patients included in the full INNOVATE cohort, 90 patients reached inclusion criteria for this study **(Figure 1**). Inclusion criteria included: Patients from INNOVATE whom gave appropriate consent, underwent a diagnostic mpMRI of the prostate at UCLH which indicated them for prostate biopsy, plus a subsequent biopsy at UCLH in which the targets were cognitively influenced by mpMRI and a diagnosis of prostate cancer was made. Patients were excluded if they had a prior cancer diagnosis and were having a biopsy for restaging or for active surveillance.

Patient Inclusion Criteria
1. Men referred to our center for prostate mp-MRI following biopsy elsewhere
2. Biopsy naive men presenting to our institution with a clinical suspicion of prostate cancer
Patient Exclusion Criteria
1. Men unable to have a MRI scan, or in whom artifact would reduce quality of MRI
2. Men unable to given informed consent
3. Previous treatment (prostatectomy, radiotherapy, brachytherapy) of prostate cancer
4. On-going hormonal treatment for prostate cancer
5. Previous biopsy within 6 months of scheduled mp-MRI
Withdrawal criteria
1. Images inadequate for analysis due to artifact or image acquisition problems even after a repeat scan

Table 1: Inclusion, exclusion and withdrawal criteria for the INNOVATE study

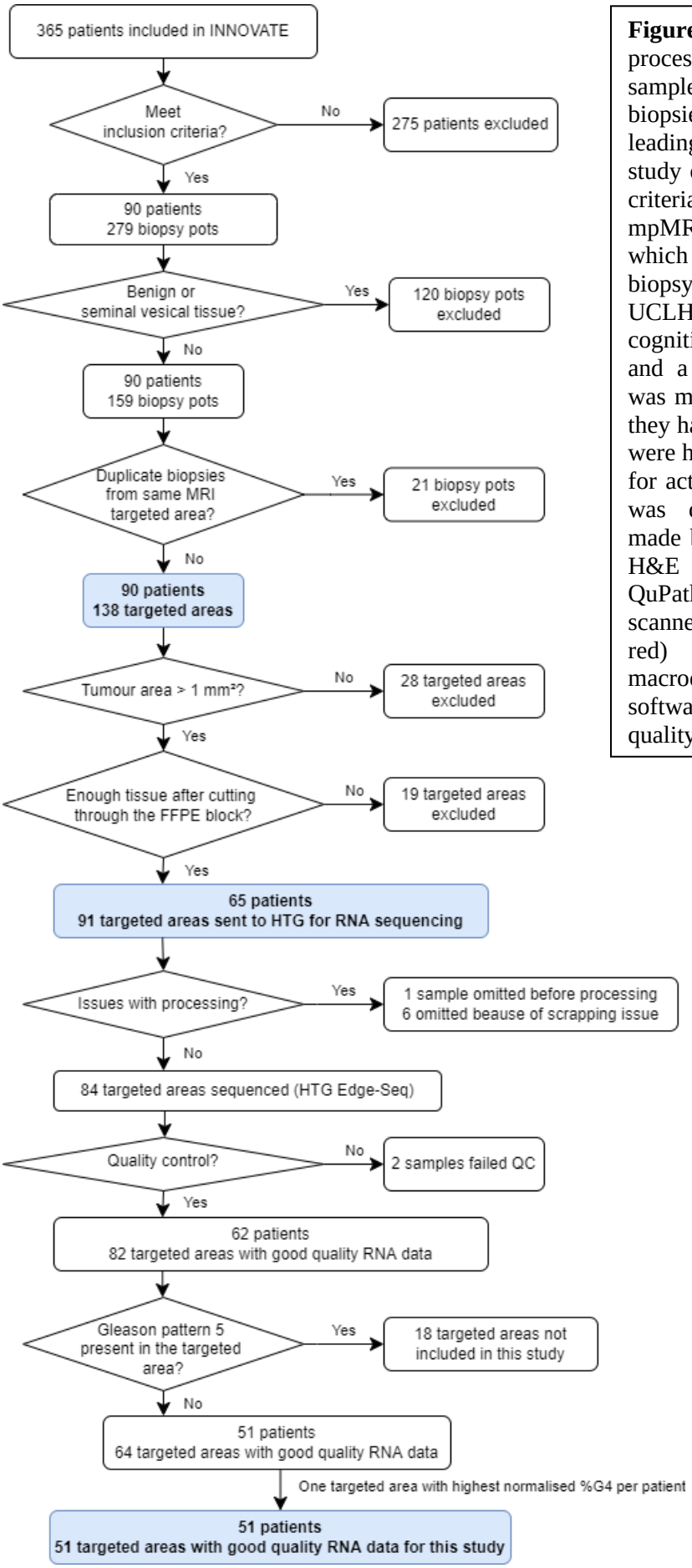

Figure 1: Flow chart describing the process of patient selection and sample selection from prostate biopsies in the INNOVATE cohort, leading to the current cohort for the study of %G4. The patient inclusion criteria include consent, diagnostic mpMRI of the prostate at UCLH which indicated them for prostate biopsy, plus a subsequent biopsy at UCLH in which the targets were cognitively influenced by mpMRI and a diagnosis of prostate cancer was made. Patients were excluded if they had a prior cancer diagnosis and were having a biopsy for restaging or for active surveillance. Tumour area was determined from annotation made by uropathologists on scanned H&E images in imaging software QuPath (see insert for an Example of scanned H&E slide, annotated (in red) by uropathologist, for macrodissection in the imaging software QuPath version 0.2.3.). QC: quality control metrics.

Tumour annotation example:

2.2.2. Prostate biopsy

Prostate biopsy was only undertaken if clinically indicated after mpMRI and MDT review. During clinical review biopsy target areas were decided, these are then indicated on a map and described in a report. In the 90 patients in this cohort all the prostate biopsies were undertaken transperineally and consisted of MRI-targeted deployments (cognitive method) only. The median (IQR) time between patient MRI and prostate biopsy was 25 days (IQR = 18 to 57). As is standard practice at our centre, prostate cores biopsied taken from each targeted area are submitted in a separate formalin containing pathology pots (biopsy pot). They are then embedded in one or two Formalin-fixed paraffin-embedded (FFPE) cassettes depending on the number of cores taken. In this cohort the 90 patients had a total of 279 biopsy pots (and therefore 279 targeted areas), from which 12 and 108 pots were excluded for containing seminal vesicle tissue and benign biopsies respectively. (**Figure 1**).

2.2.3. Digitisation and annotation of histology slides

The diagnostic hematoxylin and eosin (H&E) slides representing 138 targeted areas, selected after excluding duplicates, were manually scanned at x40 using a Hamamatsu Nanozoomer S360 (GA-MRJ, Model S360, year 2019). The scanned images were annotated by two senior uropathologists (AF, AH) for macrodissection of tumour areas. An example is shown in **Figure 1**. Contours were made using QuPath version 0.2.3 [36], an open source software platform for whole slide image analysis. Image type was set as Brightfield (H&E), contours were drawn by freehand using the click and drag polygon tool. After contours were drawn pathologists made an assessment of the overall Gleason score of the tumour in all contours for each image. In the images that contained overall Gleason score 3+4 or 4+3. A %G4 was also provided (defined as the estimated percentage of glands presenting as pattern 4 as a proportion of all tumorous glands). If a targeted area had been divided over more than one FFPE cassette, a %G4 and overall Gleason were also given for the tumour across all cassettes that represented that area. Where contours included non-biopsy core areas (i.e. surrounding white space) the QuPath wand tool was used to pull the contours tight to the outline of the core.

2.2.4. RNA sequencing

RNA sequencing with HTG EdgeSeq technology requires sequential non stained 5 µm sections that total a minimum tissue surface area of ~5mm². After contouring of the images, calculations of tumour area for contour, and total contours per cassette could then be exported from QuPath. An example on a contour is shown in **Figure 1**. 28 tumour areas were calculated as less than 1 mm² and were excluded as macrodissection would be more difficult, have more risk of benign contamination and more risk of cutting out of the tumour area (**Figure 1**). At the cutting stage, 19 targeted areas were excluded by the lab due to risk of exhausting the FFPE block or omitted after visual inspection of the cuts for not containing tissue representative of the area contoured (**Figure 1**). The average number of sections per cassette sent to HTG was 1.7 (min = 1, max = 4). Before being added to the HTG lysis buffer, the non-stained sections were macrodissected by HTG in line with the contours drawn by the uropathologists on digital H&E images (**Figure S1).** Cassettes were combined in one lysate where they represented the same targeted area. In total 91 targeted areas were sent to HTG for RNA sequencing.

The HTG EdgeSeq system (HTG Molecular Diagnostics, Inc., Tucson AZ, USA; www.htgmolecular.com) combines HTG's proprietary quantitative nuclease protection array (qNPA) chemistry with Illumina next generation sequencing (NGS) platform to enable a semi-quantitative analysis of a panel of targeted genes in a single assay [37]. Briefly, functional DNA nuclease protection probes (NPPs) flanked by universal wing sequences were used to target RNAs. Universal DNA wingmen probes were hybridized to the wings to prevent S1 nuclease digestion. S1 nuclease was added to digest excess non-hybridized DNA probes and non-hybridized RNA, leaving only NPPs hybridized to RNA fully intact and able to be amplified. Heat denaturation was used to release the protection probes from the DNA:RNA duplexes. The released DNA protection probes were then ready for amplification/barcoding, quantification and sequencing. Sequencing was performed using Illumina NextSeq platform. This method does not require traditional nucleic acid extraction, thereby significantly reducing sample input requirements, especially from formalin-fixed paraffin-embedded samples. The assay used was HTG EdgeSeq Oncology Biomarker Panel which targets 2549 genes across 24 oncology-related groups and pathways. This panel also included housekeeper genes, negative and positive controls (https://www.htgmolecular.com/assays/obp/genes).

From the 91 targeted areas sent to HTG, 7 were omitted during macrodissection. HTG post-sequencing quality control (QC) metrics detect three different sample failure modes. From the 84 samples sequenced, none had degraded RNA or poor quality of sample, 1 had insufficient read depth and 1 failed the minimal expression variability QC failure mode (**Figure 1**)**.** As this analysis focuses on Gleason 4 from the 82 targeted areas whose RNA data passed quality control, 18 were excluded for containing Gleason pattern 5 tissue. A cohort of 64 targeted areas from 51 different patients was obtained (**Figure 1**). 11 patients had more than one targeted area included. To limit genomic bias from samples coming from the same patient (**Figure S2**), the targeted area with the highest normalised %G4 was selected for each patient, so that the final cohort contained 51 targeted areas from 51 different patients.

2.2.5. Calculation of normalised Gleason 4 %

As can be seen in **Figure 1**, pathologist annotated areas for microdissection include stroma cells, but %G4 is reported as a % of glandular tissue only. In this work we normalised the reported %G4 as a proportion of the total cells that would be included in the RNA seq (both glandular and stromal cells from the contoured area). A model of how this would theoretically improve correlation of signal from RNAseq is shown in **Figure S3**. Estimated cell counts for glandular and stromal areas for each contour was calculated from the digitised H&E image using a pixel classifier that was created by training QuPath to identify the number of cells in glandular and stroma areas [36]. An example and further details of the settings used can be found in **Figure S4.** Normalised %G4 within the contoured areas was then calculated according to the following formula:

$$Normalised\ \%G4\ = Pathologist\ reported\ \%G4\ x\ \frac{number\ of\ glandular\ cells\ in\ contour}{number\ of\ total\ cells\ in\ contour}$$

2.2.6. Data processing and statistics

Gene expression analyses were based on raw counts provided by HTG.

Statistical analyses were performed with R version 4.2.1 in the Rstudio environment version 2022.07.1+554.

Differential expression analysis between two extreme subgroups (low and high %G4) was performed from raw counts with the DESeq2 package (version 1.36.0) [38]. Cut-offs for low

and high %G4 were chosen manually according to the distribution plot of %G4. P-values were adjusted for multiple testing using the Benjamini-Hochberg procedure to control the False Discovery Rate [39]. Genes with adjusted p-values below 0.05 were called differentially expressed.

Correlation analysis was then performed on the genes identified in the differential expression analysis between the normalised values of RNA expression and normalised %G4 (see above). For the correlation analysis the whole cohort (including the middle %G4 group) was tested. The hypothesis being if % Gleason 4 is biologically relevant as a continuous variable we may be able to identify some genes in which the number of RNA copies can be seen to increase linearly along with the number of G4 cells, should an association exist. For the correlation analysis, normalisation of RNA expression was done with the variance stabilization transformation available in DESeq2 package [38]. Pearson's correlation tests were performed for each differentially expressed gene and p-values of all tests were corrected by Bonferroni method to control the Family-Wise Error Rate. Correlations were considered significant if their adjusted p-values were below 0.05.

In order to see if any of these genes showed enrichment for certain cellular pathways, enrichment analysis by over-representation was also performed in R using the ClusterProfiler package version 4.4.4 [40] with updated databases from msigdbr version 7.5.1 [41]. The chosen universe was the list of HTG genes for which entrez ID were found in Hallmark and Reactome, or th whole database of Hallmark and Reactome. Only gene sets with more than 30 genes and less than 500 genes were considered. Over-Representation analysis (ORA) looked for gene sets (e.g. pathways) over-represented (enriched) in the input list. In this study, the input list was the list of differentially expressed genes. ORA was performed with one-sided version of Fisher’s exact tests (p-value calculation based on hypergeometric distribution).

2.3. Results

2.3.1. Patients characteristics in this study

The characteristics of patients included in this study are detailed in **Table 2**. The median (IQR) time between their PSA test and mpMRI was -9 days (-25 to 17). The median time between mpMRI and prostate biopsy was 29 days (18-59). The median PSA level was 6.8 ng/ml (IQR 4.9-9.9). Most of these men (47.11%) received whole gland treatment (prostatectomy or radiotherapy), 14 (27.5%) were treated with focal therapy (high intensity focused ultrasound, cryotherapy), 8 men (16%) underwent active surveillance, 4 patients (7.9%) received hormonotherapy only or chemotherapy, and 3 (5.9%) men were lost to follow up. All patients had a suspicious lesion on MRI with a Likert score ≥ 3.

Patient characteristics	N = 51[1]
Age (years)	66 (60. 71)
Referral PSA (ng/ml)	6.8 (4.9. 9.9)
PSA Density (ng/ml/ml)	0.17 (0.13. 0.31)
Index lesion	
ISUP 1	1 (2%)
ISUP 2	36 (64.7%)
ISUP 3	5 (9.8%)
ISUP 4	3 (5.9%)
ISUP 5	6 (11.8%)
Most suspicious lesion on MRI	
Likert 2	0 (0%)
Likert 3	9 (17.6%)
Likert 4	24 (47.1%)
Likert 5	18 (35.3%)
Treatment strategy	
Active surveillance	8 (16%)
Focal therapy	14 (27.5%)
Whole gland treatment	24 (47.1%)
Hormonotherapy only	3 (5.9%)
Systemic therapy	1 (2.0%)
Lost to follow up	3 (5.9%)

[1] Median (IQR); n (%)

Table 2: Characteristics summary of patients whose targeted areas were included in the study of %G4.

2.3.2. Distribution of %G4 in the cohort

Most samples in this cohort were Gleason score 3+4, but 3 were Gleason 3+3. %G4 was not normally distributed in this cohort (**Figure 2**). Median normalised %G4 was 19.44 % (IQR 9.91-28.81). Normalisation helped against data discretisation and enabled the variable to become more continuous, with less ex aequo, without changing its distribution.

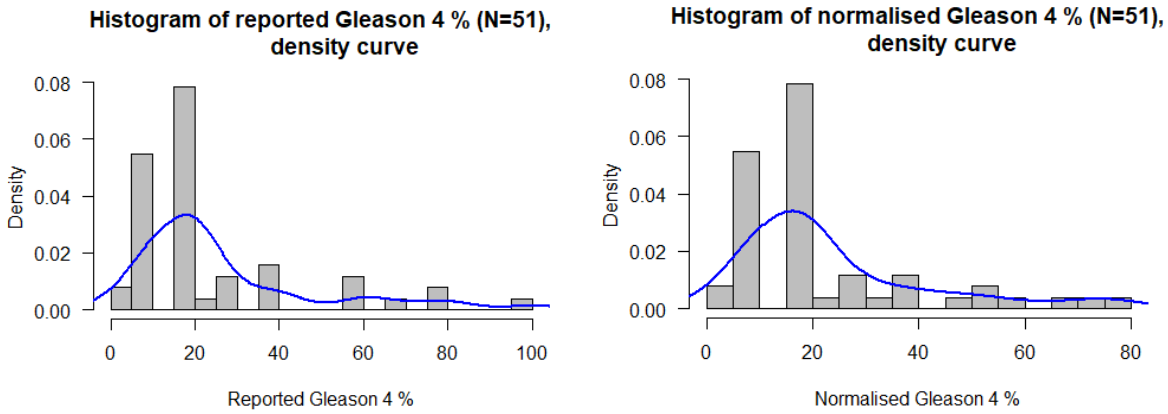

Figure 2: Histogram with density plot (blue line) representing the distribution of reported and normalised %G4 in this cohort of 51 targeted areas. Median normalised %G4 was 19.44 % (IQR 9.91-28.81). Grey bars represent number of targeted areas per %G4.

2.3.3. Genes which expression correlates with %G4

2.3.3.1. Differential expression analysis on the extremes of the cohort

Differential expression analysis was conducted on two extreme sub-groups of the cohort and included 23 targeted areas. The two groups compared were targeted areas with %G4 between 0 and 10 % (n= 16) referred to as group 0-10 and those with %G4 between 40% and 100% (n=7) referred to as group 40-100 (**Table 3**). This threshold was chosen due to the distribution of the data and recent literature questioning the traditional threshold of 50% [15,21]. Group 40-100 had longer MCCL than group 0-10, with a median of 11.0 mm (IQR: 10.0-12.5) against 3.0 mm (IQR: 2.8-5.2). Targeted areas with normalised %G4 >40% were all scored suspicious on MRI with a Likert score ≥ 3.

Differential expression analysis between groups 0-10 and 40-100 showed that 15 genes were differentially expressed with an adjusted p-value < 0.05 (**Figures 3 and 4**).

9 genes were up-regulated: SPINK1, COMP, ADAMTS1, EFNB2, ISG15, CENPN, IRS2, JAG1 and F2R, while 3 genes were down-regulated: CXCL13, BMP5 and ADRA1D (**Figures 3 and 4**). 3 other genes, HEYL, EGR1 and ENG, were significantly differentially expressed with a lower $\log_2$ fold change (**Figures 3 and 4**).

%G4 groups	**Overall**, N = 23[1]	**0-10**, N = 16[1]	**40-100**, N = 7[1]
MCCL	5.0 (3.0, 10.5)	3.0 (2.8, 5.2)	11.0 (10.0, 12.5)
Likert score			
2	1 (4.3%)	1 (6.2%)	0 (0%)
3	8 (35%)	4 (25%)	4 (57%)
4	9 (39%)	8 (50%)	1 (14%)
5	5 (22%)	3 (19%)	2 (29%)

[1] Median (IQR); n (%)

Table 3: Characteristics summary of targeted areas (N=23) included in the analysis to identify differential expressed genes. Group 0-10 included targeted areas with %G4 between 0 and 10% and group 40-100 included targeted areas with %G4 between 40 and 100%. MCCL: maximum cancer core length.

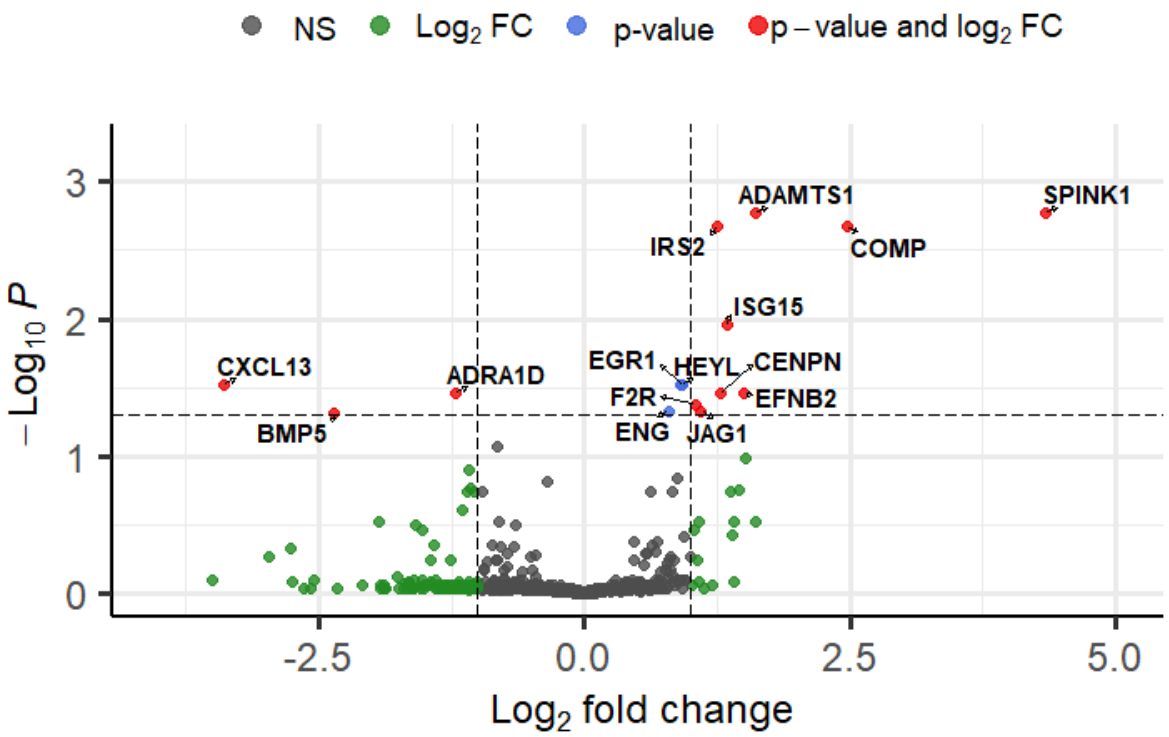

Figure 3: Volcano plot displaying differentially expressed genes between a group of targeted areas with %G4 between 0 and 10% (n=16) and a group of targeted areas with %G4 between 40 and 100% (n=7).
The vertical axis (y-axis) corresponds to the mean expression value of $\log_{10}$(adjusted p-value), and the horizontal axis (x-axis) displays the $\log_2$(fold change) value of the estimated mean value of each probe for each group after normalization. Positive x-values represent up-regulation and negative x-values represent down-regulation. The horizontal dotted line represents an adjusted p-value of 0.05. The vertical dotted line represents a $\log_2$(fold change) of –1 and 1. The red dots represent significantly differentially expressed genes with these cut-offs. The blue dots represent the probes with an adjusted p-value < 0.05 and a $\log_2$ fold change < 1. The green dots represent the probes with an adjusted p-value > 0.05 and a $\log_2$ fold change ≥ 1.

A

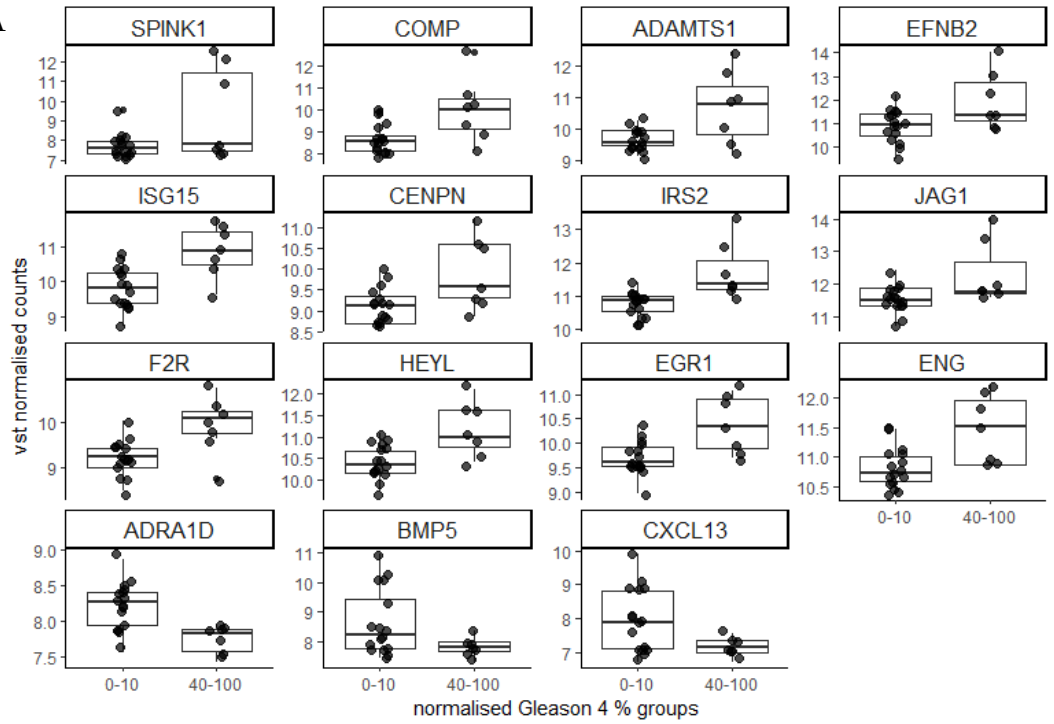

B

	Gene	Log_2 fold change	Fold change	FDR
Up-regulated	SPINK1	4,34	3,69	< 0.01
	COMP	2,47	2,10	< 0.01
	ADAMTS1	1,61	1,63	< 0.01
	EFNB2	1,51	1,58	0,03
	ISG15	1,34	1,50	0,01
	CENPN	1,29	1,47	0,03
	IRS2	1,26	1,46	< 0.01
	JAG1	1,10	1,39	0,05
	F2R	1,04	1,37	0,04
	HEYL	0,92	1,32	0,03
	EGR1	0,91	1,32	0,03
	ENG	0,79	1,27	0,05
Down-regulated	ADRA1D	-1,21	1,44	0,03
	BMP5	-2,35	2,03	0,05
	CXCL13	-3,39	2,77	0,03

Figure 4: Genes differentially expressed with an adjusted p-value < 0.05 and between a group with %G4 between 0 and 10% (0-10) and with %G4 between 40 and 100% (40-100). Box plots (A) representing down-regulated and up-regulated probes described in table below (B). Median is represented by a black line and IQR by a box. vst normalised counts: counts normalised through variance stabilization transformation representing gene expression. FDR: false discovery rate (Benjamini and Hochberg). Fold change in absolute value for up-regulated and down-regulated genes.

2.3.3.2. Correlation between gene expression and %G4 as a continuous variable

Our hypothesis is that binarizing or grouping patients via discrete %G4 thresholds may mean we are missing key biological insights. % Gleason 4 may be more relevant to the underlying biology if kept as a continuous variable. If this is true, we should be able to identify those genes for which the number of RNA copies will increase as the proportion of Gleason pattern 4 cells increase in the sequenced sample.

To investigate this correlation, analyses were carried out on the 15 genes identified in the differentially expression analysis. Pearson correlation tests identified 5 genes with expression significantly correlated to %G4 (adjusted p-value < 0.05 with Bonferroni's method): ADAMTS1, EFNB2, EGR1, IRS2, SPINK1 (**Figure 5**). They correlation coefficients were between 0.41 and 0.56, which can be deemed fair to moderate [42–44].Those genes must play a significant role in %G4 increase as they were found to be linked to %G4 through both differential expression and correlation analyses.

Person's correlation test was also carried out on all genes, but none had an adjusted p-value < 0.05 with Bonferroni's method.

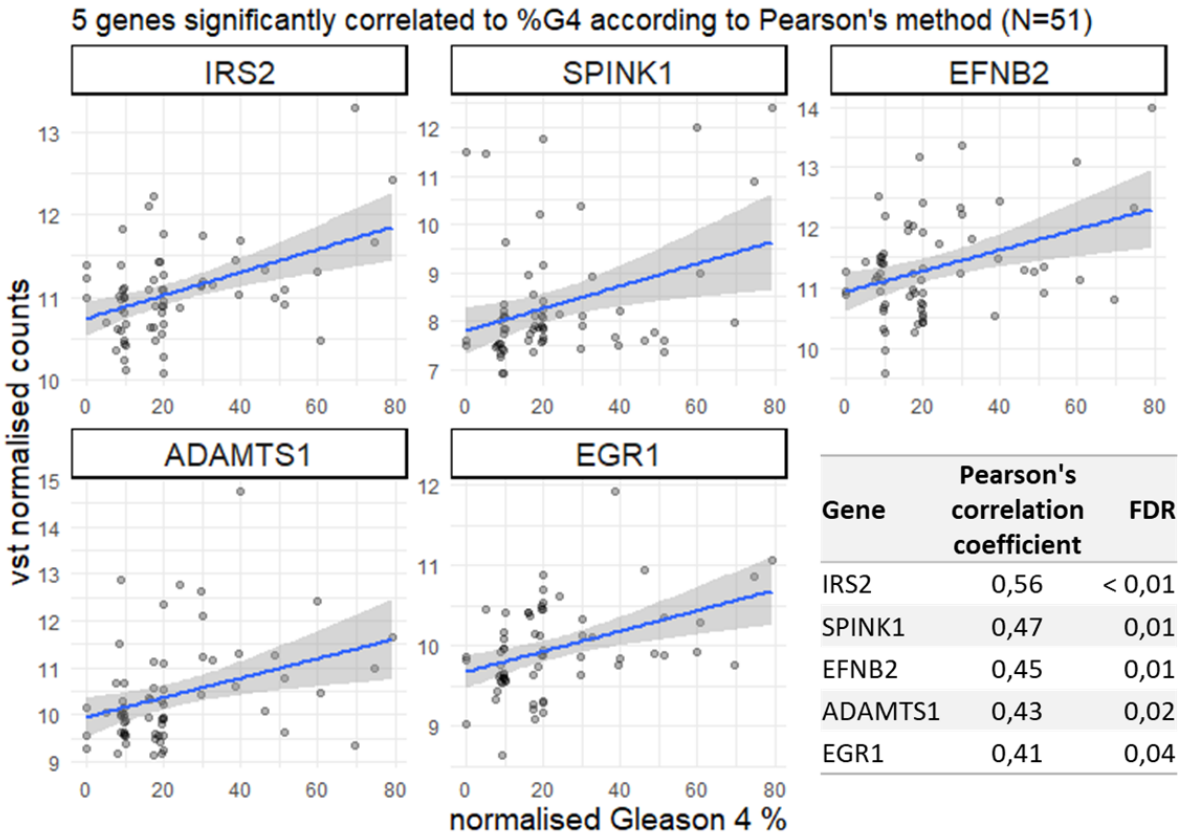

Gene	Pearson's correlation coefficient	FDR
IRS2	0,56	< 0,01
SPINK1	0,47	0,01
EFNB2	0,45	0,01
ADAMTS1	0,43	0,02
EGR1	0,41	0,04

Figure 5: Correlation plots of the 5 genes significantly correlated to normalised %G4 (adjusted p-value < 0.05 according to Bonferroni) from the 15 genes identified through differential expression, and their Person's correlation coefficients. N=51. FDR: false discovery rate (Bonferroni). vst normalised counts: counts normalised through variance stabilization transformation representing gene expression.

2.3.4. Enrichment analysis by over-representation

To establish metabolic pathways that may play significant biological roles in the increase of %G4, enrichment analysis was performed.

Hallmark gene set contains 50 gene sets. 1378 of the 2559 genes present in HTG EdgeSeq Oncology Biomarker Panel matched with a gene set. 4 of the 15 significant genes were not found (SPINK1, EFNB2, BMP5 and ADRA1D). As shown in **Figure 6**, the pathways involved with %G4 with the lowed FDR were androgen response and TNFα signaling via NFκB. Cell signalling and immune response, as well as cellular responses to stimuli (hypoxia, apoptosis, glycolysis) were over-represented in Hallmark gene set.

Reactome is an open-source, open access, manually curated and peer-reviewed pathway database containing 1615 gene sets. 2125 of the 2559 genes present in HTG EdgeSeq Oncology Biomarker Panel matched with a gene set. 3 of the 15 significant genes were not found (SPINK1, BMP5 and ADRA1D). As shown in **Figure 6**, the pathways involved with %G4 with the lowed FDR were interferon alpha beta signaling, signaling by NOTCH1, and class A1 rhodopsin like receptor, one of the largest groups of G-protein-coupled receptors which are transmembrane receptors. Cell signalling pathways via interferon and NOTCH, and cellular responses to extracellular stimuli were over-represented in Reactome gene set.

Androgen signaling as well as signalling via NOTCH, interferon and TNFα were also over-represented in the whole Hallmark and Reactome gene sets, where the universe studied was not limited to genes from HTG EdgeSeq Oncology Biomarker Panel (**Figure 7**).

ORA was also performed using the list of 5 genes correlated to %G4 as a continuous variable (Pearson's test) in the universe of HTG EdgeSeq Oncology Biomarker Panel. Interferon signaling was a common pathway found (**Figure S5**).

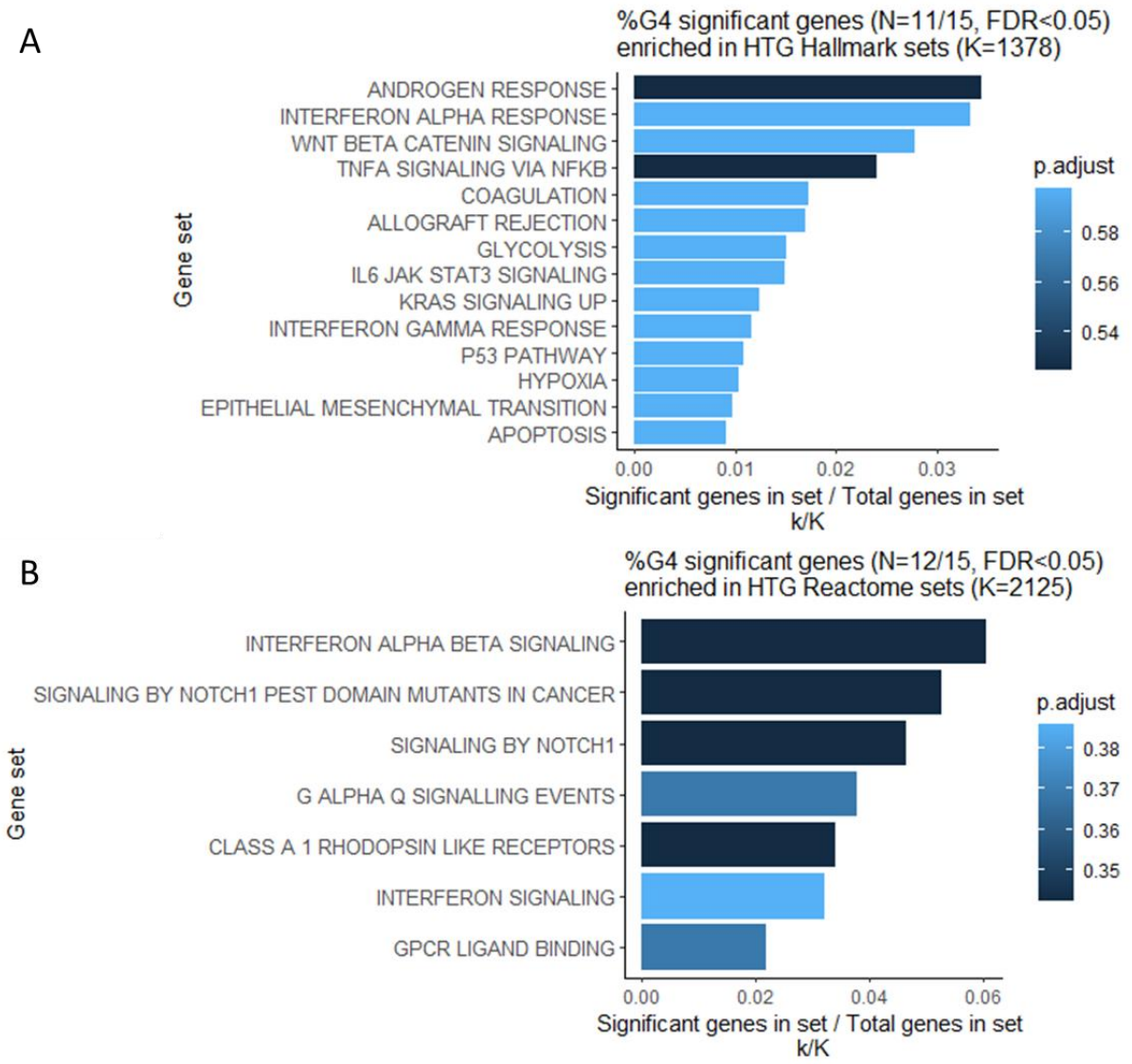

Figure 6: Barplots representing over represented gene sets by genes identified to be correlated to normalised %G4 by differential analysis (%G4 significant genes), in Hallmark (A) and Reactome (B) databases. The universe was limited to genes from HTG EdgeSeq Oncology Biomarker Panel, which entrez gene ID was found in those databases (K). p.adjust: false discovery rate (FDR). Only the gene sets with lowest p.adjust were represented.

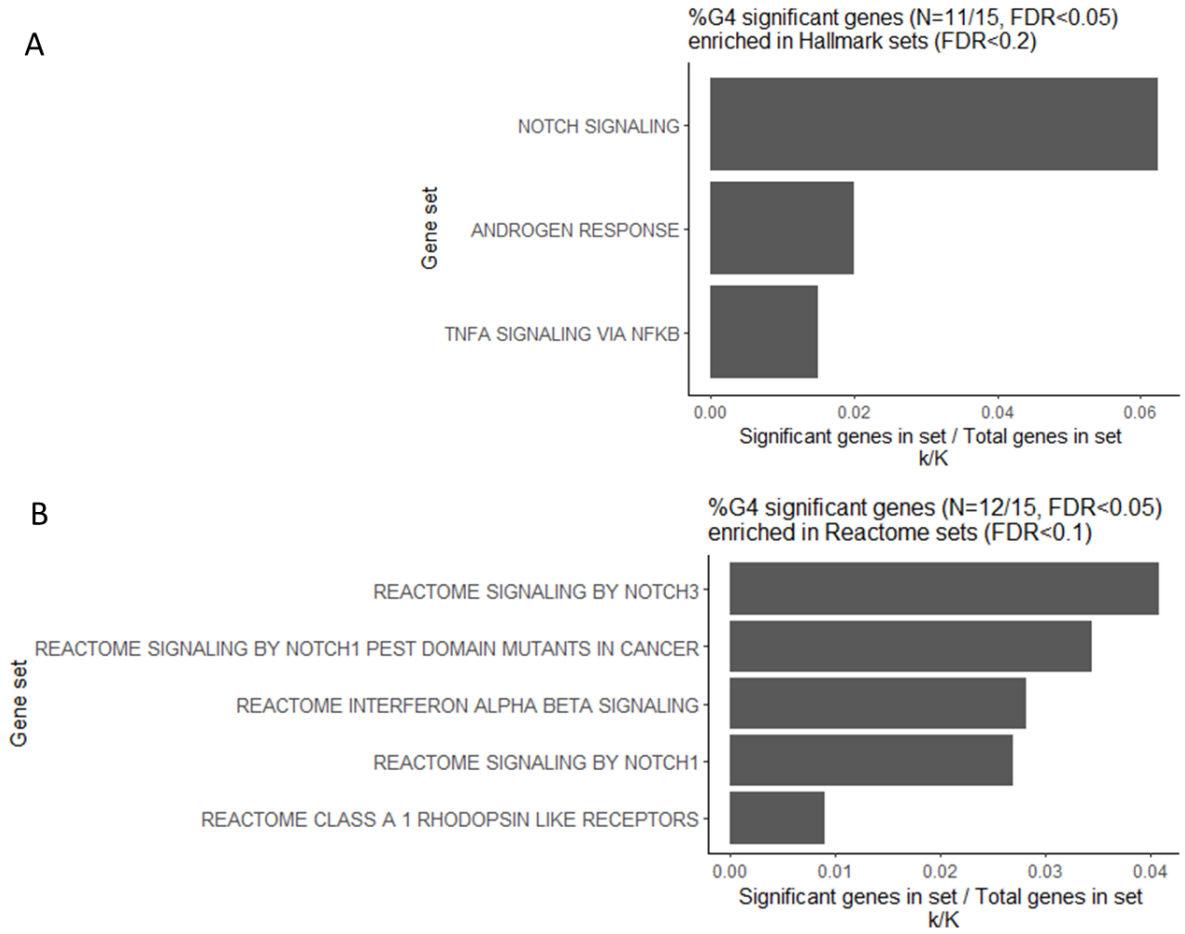

Figure 7: Barplots representing over represented gene sets by genes identified to be correlated to normalised %G4 by differential analysis (%G4 significant genes), in Hallmark (A) and Reactome (B) databases. The universe was the entire database. FDR: false discovery rate. Only the gene sets with lowest p.adjust were represented.

2.4. Discussion

This pilot study within a diagnostic cohort of 51 MRI-targeted prostate biopsies from different patients, enabled us to identify, though differential expression analysis and Pearson's correlation method, 15 genes whose expression was linked to %G4 (SPINK1, COMP, ADAMTS1, EFNB2, ISG15, CENPN, IRS2, JAG1, F2R, CXCL13, BMP5, ADRA1D, HEYL, EGR1 and ENG) from a panel of preselected oncological biomarkers. Overrepresentation analysis of these genes in the Hallmark and Reactome databases identified some metabolic pathways involved in Gleason grade 4 expansion.

In this work, we considered the stomal cell component of the cell mixture undergoing RNA sequencing in our %G4 consideration, rendering %G4 data more continuous than reported by deciles. Our hypothesis that some pathways were linearly correlated to %G4 was verified as we found 5 genes which expression was significantly correlated to %G4 with Pearson's test when tested among the genes identified through differential expression. We however did not find any when tested in the whole HTG EdgeSeq panel as adjusted p-value for multitesting were > 0.05, which could be linked to a small cohort. We however decided to prioritize a clean cohort without genomic bias by selecting only one sample per patient.

Moreover, this cohort lacks matched numbers of samples with higher and lower %G4, with lower %G4 being over represented. This was probably partially due to the study design which included patients who were referred to UCLH for mpMRI following negative biopsies elsewhere, demonstrating smaller and less aggressive disease. However, this reflects clinical reality where Gleason score 7 biopsies tend to be mostly represented by Gleason score 3+4 and fewer Gleason score 4+3. In the larger cohort of the European Randomised Study of Screening for Prostate Cancer (ERSPC) section Rotterdam [45,46], of the total 1031 biopsies, 310 were Gleason 3+4 and 104 were Gleason 4+3. The greater %G4 are only represented by a few samples, which make the confidence region larger. The variability we observed around %G4 of 20% could be also observed for higher %G4. The upper quantile of the %G4 spectrum is only represented by a few samples, which could be close to the actual average for this group or could be outliers. Thus, confidence intervals are broader for %G4 close to 100%. There could be variability in gene expression which were not represented.

Nevertheless, the strength of this cohort was to be MRI-targeted prostate biopsies. MRI enables accurate sampling [47]. Spatially resolved transcriptomics [48] led to a study from Erickson et al. which results suggest a model for how genomic instability arises in histologically benign tissue that may represent early events in cancer evolution [49]. This hints that sampling error of low %G4 in the periphery of a significant lesion with potential for high grade-disease in its genome could lead to expression levels being comparable to high %G4 samples. Thus, accurate lesion sampling is essential to interpret genomic expression linked to %G4. With MRI-targeted prostate biopsies, it is also possible to study less aggressive lesions with lower %G4 from patients who might not undergo prostatectomy [8,10]. This allowed for the analysis of %G4 as a continuous variable.

Georgescu et al. identified 9 genes from a preselected panel, FOXO1, GPD2, SPARC, HK2, COL1A2, ALDOA, SLC16A4 (MCT4), NRF2, and ATG5, which were differentially expressed Gleason pattern 3 and 4. The matching pathways involved “gluconeogenesis,” “hexose catabolic process,” and “monosaccharide catabolic process” [31], which were not significant pathways overrepresented with the genes we identified.

Contrary to the dichotomy Gleason 3 versus Gleason 4, we identified pathways related to the increase of Gleason 4 pattern, some of which were known to be involved with cancer aggressivity. The most relevant pathways associated with those genes included androgen signaling, signaling by NOTCH, interferon and TNFα.

Signal transduction through interferon alpha is linked to proliferation of prostate cancer in bones, with the loss of tumor-intrinsic type I IFN [50]. This prompted a pilot study on intra-prostatic injection of interferon-α for Gleaons 6 to 8 localised prostate cancers [51].

NFκB stimulates cell proliferation and prevents apoptosis, and promotes tumor metastasis [52]. Its transduction pathway was studied in prostate cancer [53,54].

The NOTCH gene family consists of evolutionarily conserved transmembrane receptors. NOTCH signaling pathway plays a key role in control of cell fate, stem cell potential and differentiation, proliferation, survival and migration [55].

Bin Hafeez et al. found that levels of NOTCH1 protein were higher in Gleason pattern 4 compared to Gleason pattern 3 disease, and associated with cell invasion properties [56]. Ross et al. (2011) also found up-regulation of NOTCH pathway members in Gleason 4+4=8 prostate cancer compared to Gleason 3+3=6, through the identification of 670 genes differentially expressed between those two groups, in a cohort of micro-dessected prostate

cancer cells from the radical prostatectomy specimens of 23 men [57]. Expression of NOTCH3 in prostate tumor specimens is inversely associated with survival [58].
However, there is a certain duality as NOTCH signaling can also antagonize growth and survival of both benign and malignant prostate cells, possibly through antagonistic effects of the NOTCH target HEY1 on androgen receptor function [59].
NOTCH signaling might also be involved in juxtracrine (contact-dependent) signalling between leader cells and followers in the emergence of invasive clusters, leading to a metastatic cascade [60].
This corroborates the idea that %G4 is linked to aggressivity and makes NOTCH pathway a drug target. NOTCH pathway inhibitors have been developed. The most widely used are gamma-secretase inhibitors [59]. In prostate cancer, inhibition of the NOTCH pathway enhances the anti-tumor effect of docetaxel in prostate cancer stem-like cells and suggest that NOTCH inhibition may have clinical benefits [61]. Inhibition of NOTCH pathway might also enhance the efficacy of anti-adrogen therapies, especially in castration-resistant prostate cancer [62,63].

Our results were similar to a study from Ross et al. [57] who conducted differential expression analysis between micro-dissected cancer cells from low grade (Gleason $3 + 3 = 6$) or high grade ($4 + 4 = 8$) prostate cancer in a cohort of 23 prostatectomies. Functional themes associated with Gleason grade included developmental processes, signal transduction, chemokine and embryonic stem cell pathways with specific enrichment of the androgen receptor, EGFR, TNFα, and NOTCH signaling cascades [57]. Despite having two groups of mixed Gleason 3 and 4, we found the same pathways involved with high grade prostate cancer. Additionally, we were able to show results coherent with existing literature in a cohort of MRI-targeted biopsies, which allowed to take into account low %G4. It hints that the activation or inhibition of those pathways may follow %G4 in a linear manner, which indicates we should continue to consider %G4 as a continuous variable and not a binary one, no matter the threshold [15].

2.5. Conclusion and perspectives

This pilot study, carried in a diagnostic cohort of mpMRI targeted prostate biopsies, was able to find transcriptomic changes correlated with increased %G4. It enabled a better understanding of the pathways involved with the increase of Gleason pattern 4 and managed to identify 15 genes linked to it, from a panel of preselected oncology biomarkers.

The pathways we identified yield a biological significance. The up-regulated NOTCH pathway is associated with a more aggressive disease, with a propensity for prostate cancer cells to be more invasive. This supports the importance of %G4 as a marker of aggression, which could be included in prediction models for risk stratification.

Knockdown of this pathway was found in vitro to alleviate drug resistance to chemotherapy or anti-androgen therapy. Targeting this pathway could lead to improved management of a subgroup of Gleason score 7 prostate cancers, a rather heterogeneous risk group.

As the size of our cohort was limited, it would be interesting to carry the same type of analysis on a bigger cohort with transcriptomic data available, to corroborate our findings.

Another step would be to study proteins involved in the identified pathways, for example through immunohistochemistry staining, on the same cohort to verify if the association remains.

3. DISCUSSION GENERALE

Cette étude pilote au sein d'une cohorte diagnostique de 51 biopsies prostatiques ciblées par IRM chez différents patients nous a permis d'identifier, par analyse d'expression différentielle et méthode de corrélation de Pearson, 15 gènes liés u %G4 (SPINK1, COMP, ADAMTS1, EFNB2, ISG15, CENPN, IRS2, JAG1, F2R, CXCL13, BMP5, ADRA1D, HEYL, EGR1 et ENG) à partir d'un panel de biomarqueurs oncologiques présélectionnés. L'analyse de la surreprésentation de ces gènes dans les bases de données Hallmark et Reactome a identifié certaines voies métaboliques impliquées dans l'expansion de grade 4 de Gleason.

Dans ce travail, nous avons considéré la proportion de cellules glandulaires du mélange cellulaire subissant le séquençage de l'ARN dans notre évaluation du %G4, rendant les données %G4 plus continues que celles rapportées par les déciles. Notre hypothèse selon laquelle certaines voies étaient linéairement corrélées à% G4 a été vérifiée car nous avons trouvé 5 gènes dont l'expression était significativement corrélée à% G4 avec le test de Pearson lorsqu'ils étaient testés parmi les gènes identifiés par expression différentielle. Cependant, nous n'en avons trouvé aucun lors des tests sur l'ensemble du panel HTG EdgeSeq, car la valeur p ajustée pour les tests multiples était > 0,05, ce qui pourrait être lié à une petite cohorte. Nous avons cependant décidé de privilégier une cohorte propre sans biais génomique en sélectionnant un seul échantillon par patient.

De plus, cette cohorte manque de nombres appariés d'échantillons entre un %G4 élevé et bas, le %G4 bas étant surreprésenté. Cela était probablement dû en partie à la conception de l'étude qui incluait des patients référés à l'UCLH pour une IRMmp après des biopsies négatives ailleurs, démontrant une maladie plus petite et moins agressive. Cependant, cela reflète la réalité clinique où les biopsies au score de Gleason 7 ont tendance à être principalement représentées par le score de Gleason 3 + 4 et moins le score de Gleason 4 + 3 [45,46]. Les %G4 élevés ne sont représentés que par quelques échantillons, ce qui agrandit l’intervalle de confiance. La variabilité que nous avons observée autour de %G4 de 20% pourrait également être observée pour des %G4 plus élevés. Le quantile supérieur du spectre %G4 n'est représenté que par quelques échantillons, qui pourraient être proches de la moyenne réelle pour ce groupe ou pourraient être des valeurs aberrantes. Ainsi, les intervalles de

confiance sont plus larges pour %G4 proche de 100%. Il pourrait y avoir une variabilité dans l'expression des gènes qui n'était pas représentée.

Néanmoins, la force de cette cohorte était de n'inclure que des biopsies de la prostate ciblées par IRM. L'IRMmp permet un meilleur échantillonnage [47] La transcriptomique de résolution spatiale [48] a conduit à une étude d'Erickson et al. dont les résultats suggèrent un modèle sur la façon dont l'instabilité génomique se produit dans un tissu histologiquement bénin qui peut représenter des événements précoces dans l'évolution vers le cancer [49]. Cela laisse entendre qu'une erreur d'échantillonnage de faible %G4 à la périphérie d'une lésion significative avec un potentiel de maladie de haut grade dans son génome, pourrait conduire à des niveaux d'expression comparables à des échantillons de %G4 élevé. Ainsi, l'échantillonnage précis des lésions est essentiel pour interpréter l'expression génomique liée au %G4. Avec les biopsies prostatiques ciblées par IRM, il est également possible d'étudier des lésions moins agressives avec un %G4 inférieur chez des patients qui pourraient ne pas subir de prostatectomie [8,10]. Cela a permis l'analyse de %G4 comme une variable continue.

Georgescu et al. a identifié 9 gènes à partir d'un panel présélectionné, FOXO1, GPD2, SPARC, HK2, COL1A2, ALDOA, SLC16A4 (MCT4), NRF2 et ATG5, qui étaient exprimés de manière différentielle Gleason pattern 3 et 4. Les voies correspondantes impliquaient la « gluconéogenèse », « l'hexose processus catabolique » et « processus catabolique des monosaccharides » [31], qui n'étaient pas des voies significatives surreprésentées avec les gènes que nous avons identifiés.
Contrairement à la dichotomie Gleason 3 versus Gleason 4, nous avons identifié des voies liées à l'augmentation du grade de Gleason 4, dont certaines étaient connues pour être impliquées dans l'agressivité du cancer. Les voies les plus pertinentes associées à ces gènes comprenaient la signalisation androgénique, la signalisation par NOTCH, interféron et TNFα.

La transduction du signal par l'interféron α est liée à la prolifération du cancer de la prostate dans les os, avec la perte d'IFN de type I intrinsèque à la tumeur [50]. Cela a conduit à une étude pilote sur l'injection intra-prostatique d'interféron α pour les cancers de prostate localisés de Gleaons 6 à 8 [51].
Le NFκB stimule la prolifération cellulaire et prévient l'apoptose, et favorise la métastase tumorale [52]. Sa voie de transduction a été étudiée dans le cancer de la prostate [53,54].

La famille de gènes NOTCH est constituée de récepteurs transmembranaires conservés au cours de l'évolution. La voie de signalisation NOTCH joue un rôle clé dans le contrôle du destin cellulaire, du potentiel et de la différenciation des cellules souches, de la prolifération, de la survie et de la migration [55]. Bin Hafeez et al. ont constaté que les niveaux de protéine NOTCH1 étaient plus élevés dans le Gleason 4 par rapport au Gleason 3, et associés à des propriétés d'invasion cellulaire [56]. Ross et al. (2011) ont également trouvé une régulation à la hausse des membres de la voie NOTCH dans le cancer de la prostate Gleason 4 + 4 = 8 par rapport à Gleason 3 + 3 = 6 [57]. L'expression de NOTCH3 dans les échantillons de tumeurs de la prostate est inversement associée à la survie [58]. La signalisation NOTCH pourrait également être impliquée dans la signalisation juxtracrine (dépendante du contact) entre les cellules leader et les suiveurs dans l'émergence de clusters invasifs, conduisant à une cascade métastatique [60]. Cela corrobore l'idée que le %G4 est lié à l'agressivité et fait de la voie NOTCH une cible médicamenteuse. Des inhibiteurs de la voie NOTCH ont été développés. Les plus utilisés sont les inhibiteurs de la gamma-sécrétase [59]. Dans le cancer de la prostate, l'inhibition de la voie NOTCH renforce l'effet antitumoral du docétaxel dans les cellules souches du cancer de la prostate et suggère que l'inhibition de NOTCH pourrait avoir des avantages cliniques [61]. L'inhibition de la voie NOTCH pourrait également améliorer l'efficacité des thérapies anti-adrogènes, en particulier dans le cancer de la prostate résistant à la castration [62,63].

Nos résultats étaient similaires à une étude de Ross et al. [57] qui ont effectué une analyse d'expression différentielle entre les cellules cancéreuses micro-disséquées d'un cancer de la prostate de bas grade (Gleason 3 + 3 = 6) ou de haut grade (4 + 4 = 8) dans une cohorte de 23 prostatectomies. Les thèmes fonctionnels associés au grade de Gleason comprenaient les processus de développement, la transduction du signal, les voies des chimiokines et des cellules souches embryonnaires avec un enrichissement spécifique du récepteur aux androgènes, des cascades de signalisation EGFR, TNFα et NOTCH [57]. Malgré deux groupes de Gleason 3 et 4 mixtes, nous avons trouvé les mêmes voies impliquées dans le cancer de la prostate de haut grade. De plus, nous avons pu montrer des résultats cohérents avec la littérature existante dans une cohorte de biopsies ciblées par IRM, ce qui a permis de prendre en compte un faible %G4. Cela laisse entendre que l'activation ou l'inhibition de ces voies peuvent suivre %G4 de manière linéaire, ce qui indique qu'il faut continuer à considérer %G4 comme une variable continue et non binaire, quel que soit le seuil [15].

4. PERSPECTIVES

La taille de notre cohorte étant limitée, il serait intéressant de porter le même type d'analyse sur une plus grande cohorte avec des données transcriptomiques disponibles, pour corroborer nos résultats.

Une autre étape consisterait à étudier les protéines impliquées dans les voies identifiées, par exemple par coloration immunohistochimique, sur la même cohorte pour vérifier si l'association persiste.

Cette cohorte INNOVATE comporte par ailleurs l'association des %G4, des données transcriptomiques et radiomiques dans le cadre du protocole IRM VERDICT (Vascular and Extracellular Restricted Diffusion for Cytometry in Tumours, soit restriction de diffusion vasculaire et extracellulaire pour la cytométrie dans les tumeurs) [33], permettant d'étudier les gènes liés à la visibilité du cancer de prostate par l'intermédiaire du coefficient apparent de diffusion (ADC) par exemple.

5. CONCLUSION

Cette étude pilote, menée dans une cohorte diagnostique de biopsies de la prostate ciblées par IRMmp, a pu trouver des changements transcriptomiques corrélés à une augmentation du %G4. Elle a permis une meilleure compréhension des voies impliquées dans l'augmentation du grade de Gleason 4 et sommes parvenus à identifier 15 gènes qui lui sont liés, à partir d'un panel de biomarqueurs oncologiques présélectionnés.

Les voies que nous avons identifiées ont une signification biologique. La voie NOTCH régulée à la hausse est associée à une maladie plus agressive, avec une propension des cellules cancéreuses de la prostate à être plus invasives. Cela confirme l'importance de %G4 en tant que marqueur d'agressivité, qui pourrait être inclus dans les modèles de prédiction pour la stratification des risques.

Le renversement de cette voie a été trouvé in vitro pour atténuer la résistance aux médicaments à la chimiothérapie ou à la thérapie anti-androgène. Cibler cette voie pourrait conduire à une meilleure prise en charge d'un sous-groupe de cancers de la prostate de score de Gleason 7, un groupe à risque plutôt hétérogène.

6. FIGURES SUPPLEMENTAIRES

	Low risk	*Intermediate risk*	*High risk*
Criteria	PSA ≤ 10 and	PSA >10–20 or	PSA > 20 or
	GS ≤6 and	GS 7 (ISUP 2–3) or	GS >7 (ISUP 4–5) or
	cT1c-2a	cT2b	cT2c

Table S1: **Criteria common to the following prostate cancer risk stratification systems:** D'Amico/Association Francaise d'Urologie (2020), European Association of Urology (2021), National Institute for Health and Care Excellence or NICE (2019). cT: clinical tumour stage. GS: Gleason score. PSA: prostate-specific antigen, in ng/mL.

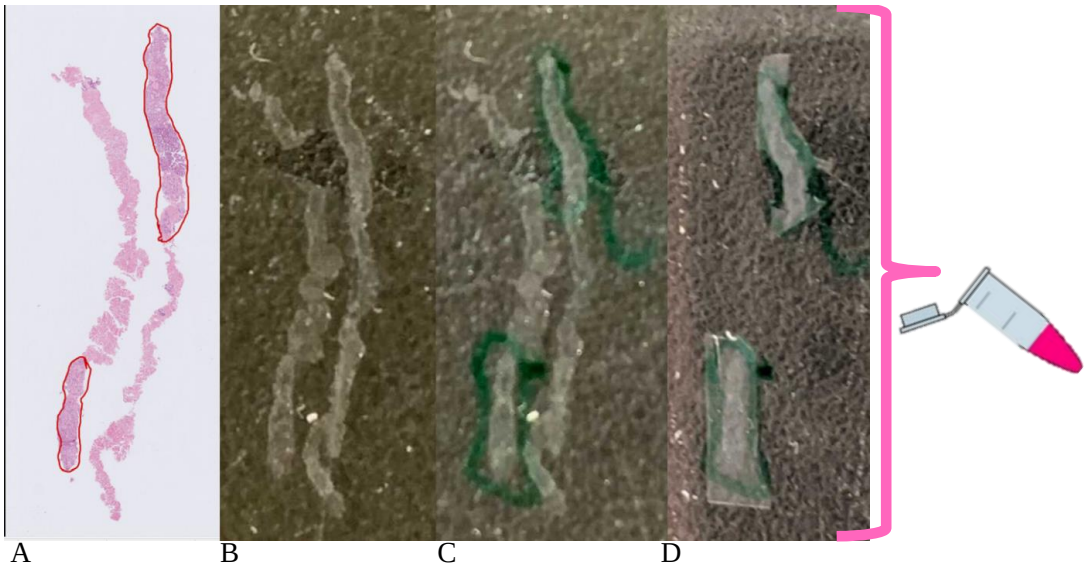

Figure S1: Example of sample processing by HTG. The FFPE unstained slides (B) were marked up (C) macrodissected (D) based on annotations drawn on the digitised H&E images (A), before being added to the HTG lysis buffer.

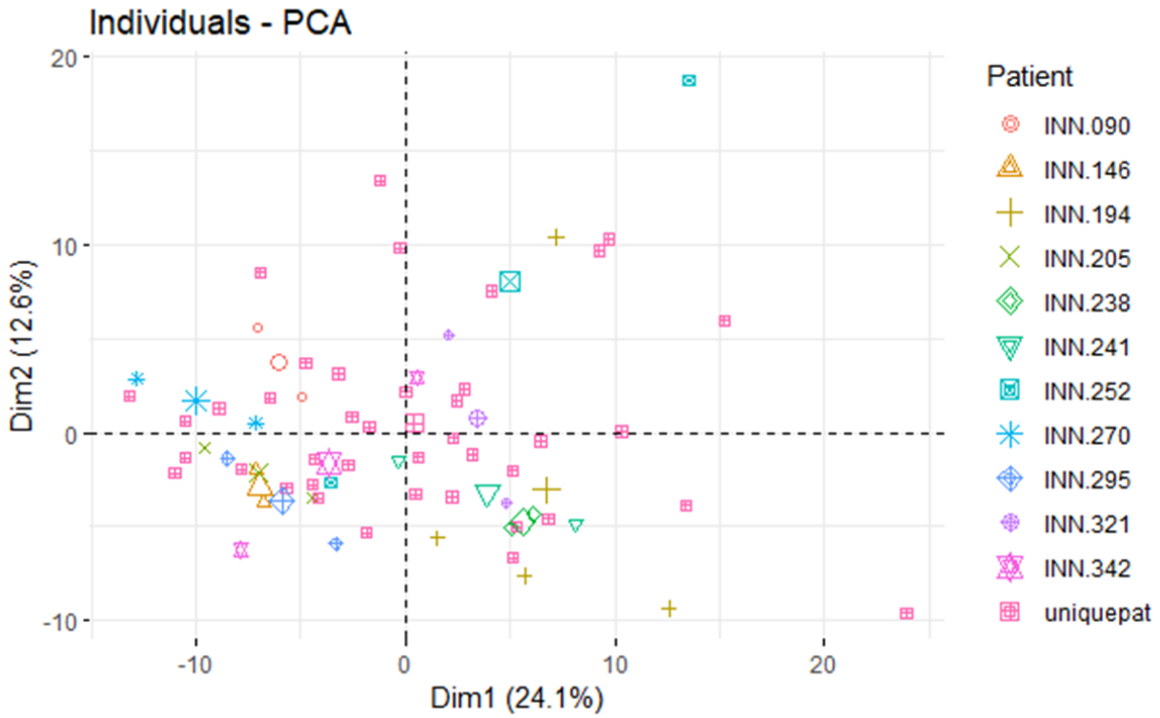

Figure S2: Principal component analysis (PCA) on the 64 targeted areas with good quality RNA for this study, from 51 different patients. 40 patients had a unique targeted area in this cohort (uniquepat), while 11 (listed in the legend) had more than one. While some samples from the same patient were not clustered (such as INN.252), others such as INN.238 were, prompting the decision to have a clean cohort without genomic bias with only one targeted area per patient.

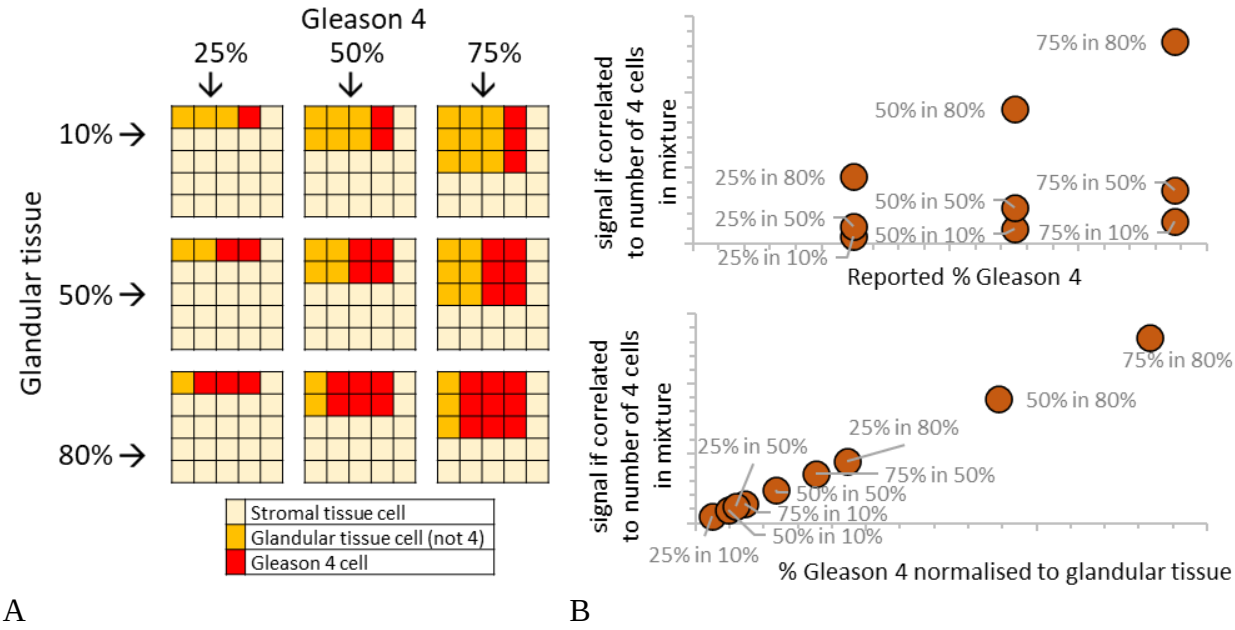

A B

Figure S3: Model for normalisation of %G4 based on gladular and stroma tissu cell proportion. Pathologist annotated areas for microdissection include stroma cells, but %4 is defined as the estimated percentage of glands presenting as pattern 4 as a proportion of all tumorous glands. In this work we attempted to normalised the reported %G4 to a proportion of the total cells that would be included in the total RNA seq cell mixture, i.e. both glandular and stromal cells from the contoured area. A simplified model including three cell types (stromal, glandular cancer (non 4), and glandular cancer Gleason 4 is shown in (A) across different proportions of glandular tissue and different reported %G4. How this would theoretically improve correlation of signal from RNAseq is shown in (B). An assumption is made that all cells contribute equally to the RNA seq data, that all glandular cells within the contoured area are cancerous and that the modelled RNAseq 'signal' shown here directly correlates in a linear manor with the number of %G4 cells in the sequenced cell mixture.

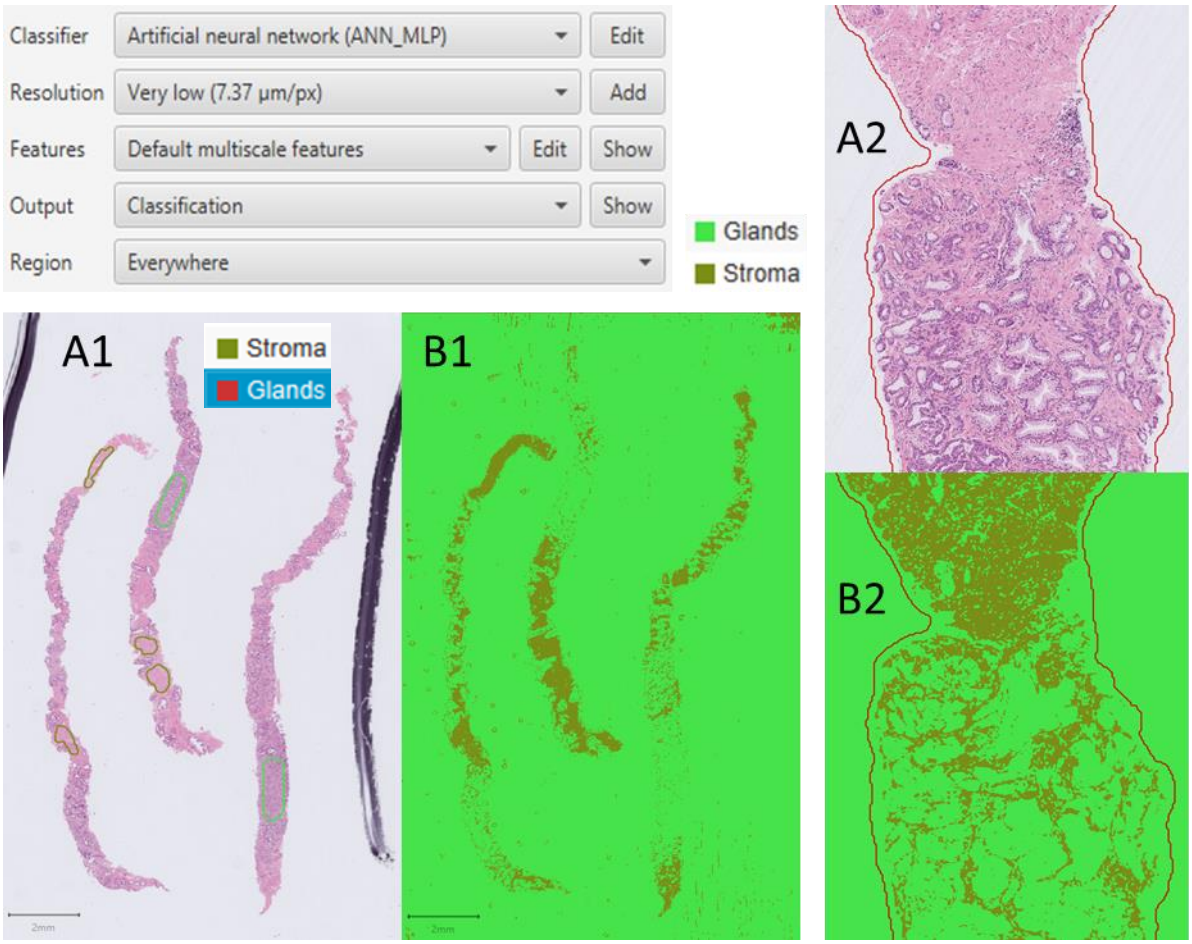

Figure S4: Settings for the Pixel classifier and example of trained pixel classifier on H&E images. A1 is an image of scanned H&E with example annotations of differents classes ("Glands" and "Stroma") which were used to train the pixel classifier. A2 is a zoomed in example of tissue before classification. The red contour in A2 and B2 represents the original tumour markup by uropathologists. The classifier once trained was saved and applied to all images within the data set. It was then used to obtain the number of cell detections of glands and stroma, within the existing contours, through an automated script using the cell detection package. When applied to the whole slide, it resulted in images as shown in B1 and B2.

The image color stain was set as: " H&E modified ", "Stain 1" : "Hematoxylin", "Values 1" : " 0.651 0.701 0.29 ", "Stain 2" : "Eosin", "Values 2" : " 0.216 0.801 0.558 ", "Background" : " 255 255 255 ".Cell counting was based on the in built cell detection package with the following settings: runPlugin('qupath.imagej.detect.cells.WatershedCellDetection', '{"detectionImageBrightfield": "Hematoxylin OD", "requestedPixelSizeMicrons": 0.5, "backgroundRadiusMicrons": 8.0, "medianRadiusMicrons": 0.0, "sigmaMicrons": 1.5, "minAreaMicrons": 10.0, "maxAreaMicrons": 400.0, "threshold": 0.1, "maxBackground": 2.0, "watershedPostProcess": true, "cellExpansionMicrons": 5.0, "includeNuclei": true, "smoothBoundaries": true, "makeMeasurements": true}'). The resolution set on very low provided better results and faster running of the script.

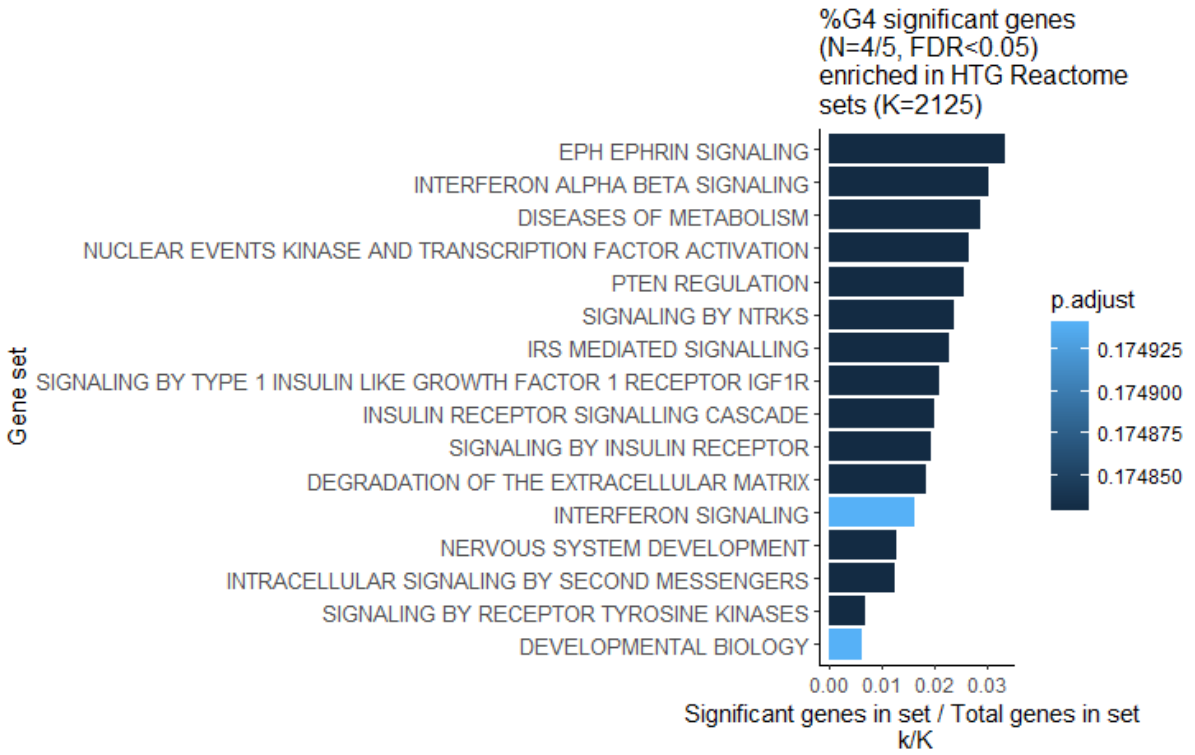

Figure S5: Barplots representing over represented gene sets by genes identified to be correlated to normalised %G4 by differential analysis and Pearson's correlation test (%G4 significant genes, only SPINK1 was not found in the database), in Reactome database. The universe was limited to genes from HTG EdgeSeq Oncology Biomarker Panel, which entrez gene ID was found in this database (K). p.adjust: false discovery rate (FDR). Only the gene sets with lowest p.adjust were represented.

REFERENCES

[1] Gleason DF. Histologic grading of prostate cancer: A perspective. *Hum Pathol* 1992;23:273–9.

[2] Srigley JR, Amin M, Boccon-Gibod L, Egevad L, Epstein JI, Humphrey PA, et al. Prognostic and predictive factors in prostate cancer: Historical perspectives and recent international consensus initiatives. *Scand J Urol Nephrol Suppl* 2005;39:8–19.

[3] Bostwick DG, Grignon DJ, Hammond MEH, Amin MB, Cohen M, Crawford D, et al. Prognostic Factors in Prostate CancerCollege of American Pathologists Consensus Statement 1999. *Arch Pathol Lab Med* 2000;124:995–1000.

[4] Epstein JI, Allsbrook WC, Amin MB, Egevad LL, Bastacky S, López Beltrán A, et al. The 2005 International Society of Urological Pathology (ISUP) consensus conference on Gleason grading of prostatic carcinoma. *Am J Surg Pathol* 2005;29:1228–42.

[5] Delahunt B, Miller RJ, Srigley JR, Evans AJ, Samaratunga H. Gleason grading: past, present and future. *Histopathology* 2012;60:75–86.

[6] Helpap B, Egevad L. The significance of modified Gleason grading of prostatic carcinoma in biopsy and radical prostatectomy specimens. *Virchows Arch 2006 4496* 2006;449:622–7.

[7] Billis A, Guimaraes MS, Freitas LLL, Meirelles L, Magna LA, Ferreira U. The Impact of the 2005 International Society of Urological Pathology Consensus Conference on Standard Gleason Grading of Prostatic Carcinoma in Needle Biopsies. *J Urol* 2008;180:548–53.

[8] Mottet N, van den Bergh RCN, Briers E, Van den Broeck T, Cumberbatch MG, De Santis M, et al. EAU-EANM-ESTRO-ESUR-SIOG Guidelines on Prostate Cancer—2020 Update. Part 1: Screening, Diagnosis, and Local Treatment with Curative Intent. *Eur Urol* 2021;79:243–62.

[9] NICE Guidance – Prostate cancer: diagnosis and management. *BJU Int* 2019;124:9–26.

[10] Rozet F, Mongiat-Artus P, Hennequin C, Beauval JB, Beuzeboc P, Cormier L, et al. Recommandations françaises du Comité de cancérologie de l'AFU – actualisation 2020–2022 : cancer de la prostate. *Progrès En Urol* 2020;30:S136–251.

[11] Epstein JI, Amin MB, Reuter VE, Humphrey PA. Contemporary gleason grading of prostatic carcinoma. *Am J Surg Pathol* 2017;41:e1–7.

[12] Humphrey PA, Moch H, Cubilla AL, Ulbright TM, Reuter VE. The 2016 WHO Classification of Tumours of the Urinary System and Male Genital Organs—Part B: Prostate and Bladder Tumours. *Eur Urol* 2016;70:106–19.

[13] Morash C, Tey R, Agbassi C, Klotz L, McGowan T, Srigley J, et al. Active surveillance for the management of localized prostate cancer: Guideline recommendations. *Can Urol Assoc J* 2015;9:171.

[14] Sharma M, Miyamoto H. Percent Gleason pattern 4 in stratifying the prognosis of patients with intermediate-risk prostate cancer. *Transl Androl Urol* 2018;7:S484.

[15] Sauter G, Steurer S, Clauditz TS, Krech T, Wittmer C, Lutz F, et al. Clinical utility of quantitative gleason grading in prostate biopsies and prostatectomy specimens. *Eur Urol* 2016;69:592–8.

[16] Huang CC, Kong MX, Zhou M, Rosenkrantz AB, Taneja SS, Melamed J, et al. Gleason score 3+4=7 prostate cancer with minimal quantity of gleason pattern 4 on needle biopsy is associated with low-risk tumor in radical prostatectomy specimen. *Am J Surg Pathol* 2014;38:1096–101.

[17] Perlis N, Sayyid R, Evans A, Van Der Kwast T, Toi A, Finelli A, et al. Limitations in Predicting Organ Confined Prostate Cancer in Patients with Gleason Pattern 4 on Biopsy: Implications for Active Surveillance. *J Urol* 2017;197:75–83.

[18] Choy B, Pearce SM, Anderson BB, Shalhav AL, Zagaja G, Eggener SE, et al. Prognostic significance of percentage and architectural types of contemporary gleason pattern 4 prostate cancer in radical prostatectomy. *Am J Surg Pathol* 2016;40:1400–6.

[19] Cole AI, Morgan TM, Spratt DE, Palapattu GS, He C, Tomlins SA, et al. Prognostic Value of Percent Gleason Grade 4 at Prostate Biopsy in Predicting Prostatectomy Pathology and Recurrence. *J Urol* 2016;196:405–11.

[20] Kir G, Seneldir H, Gumus E. Outcomes of Gleason score 3 + 4 = 7 prostate cancer with minimal amounts (<6%) vs ≥6% of Gleason pattern 4 tissue in needle biopsy specimens. *Ann Diagn Pathol* 2016;20:48–51.

[21] Bommelaere T, Villers A, Puech P, Ploussard G, Labreuche J, Drumez E, et al. Risk Estimation of Metastatic Recurrence After Prostatectomy: A Model Using Preoperative Magnetic Resonance Imaging and Targeted Biopsy. *Eur Urol Open Sci* 2022;41:24.

[22] Cheng L, Davidson DD, Lin H, Koch MO. Percentage of Gleason pattern 4 and 5 predicts survival after radical prostatectomy. *Cancer* 2007;110:1967–72.

[23] Sato S, Kimura T, Yorozu T, Onuma H, Iwatani K, Egawa S, et al. Cases Having a Gleason Score 3+4=7 with <5% of Gleason Pattern 4 in Prostate Needle Biopsy Show

Similar Failure-free Survival and Adverse Pathology Prevalence to Gleason Score 6 Cases in a Radical Prostatectomy Cohort. *Am J Surg Pathol* 2019;43:1560–5.

[24] Adams J. Transcriptome: Connecting the Genome to Gene Function | Learn Science at Scitable. *Nat Educ 1(1)195* 2008.

[25] Wang X, Li S, Wu J, Ding R, Quan J, Zheng E, et al. A Transcriptome Analysis Identifies Biological Pathways and Candidate Genes for Feed Efficiency in DLY Pigs. *Genes (Basel)* 2019;10.

[26] Vishnubalaji R, Sasidharan Nair V, Ouararhni K, Elkord E, Alajez NM. Integrated Transcriptome and Pathway Analyses Revealed Multiple Activated Pathways in Breast Cancer. *Front Oncol* 2019;0:910.

[27] Terabayashi T, Germino GG, Menezes LF. Pathway identification through transcriptome analysis. *Cell Signal* 2020;74:109701.

[28] Jhun MA, Geybels MS, Wright JL, Kolb S, April C, Bibikova M, et al. Gene expression signature of Gleason score is associated with prostate cancer outcomes in a radical prostatectomy cohort. *Oncotarget* 2017;8:43035.

[29] Kohaar I, Petrovics G, Srivastava S. A Rich Array of Prostate Cancer Molecular Biomarkers: Opportunities and Challenges. *Int J Mol Sci* 2019;20.

[30] Na R, Wu Y, Ding Q, Xu J. Clinically available RNA profiling tests of prostate tumors: utility and comparison. *Asian J Androl* 2016;18:575.

[31] Georgescu I, Gooding RJ, Doiron RC, Day A, Selvarajah S, Davidson C, et al. Molecular characterization of Gleason patterns 3 and 4 prostate cancer using reverse Warburg effect-associated genes. *Cancer Metab* 2016;4.

[32] Roberto D, Selvarajah S, Park PC, Berman D, Venkateswaran V. Functional validation of metabolic genes that distinguish Gleason 3 from Gleason 4 prostate cancer foci. *Prostate* 2019;79:1777–88.

[33] Johnston E, Pye H, Bonet-Carne E, Panagiotaki E, Patel D, Galazi M, et al. INNOVATE: A prospective cohort study combining serum and urinary biomarkers with novel diffusion-weighted magnetic resonance imaging for the prediction and characterization of prostate cancer. *BMC Cancer* 2016;16:816.

[34] Appayya MB, Adshead J, Ahmed HU, Allen C, Bainbridge A, Barrett T, et al. National implementation of multi-parametric magnetic resonance imaging for prostate cancer detection – recommendations from a UK consensus meeting. *Bju Int* 2018;122:13.

[35] Khoo CC, Eldred-Evans D, Peters M, Tanaka MB, Noureldin M, Miah S, et al. Likert vs PI-RADS v2: a comparison of two radiological scoring systems for detection of

clinically significant prostate cancer. *BJU Int* 2020;125:49–55.

[36] Bankhead P, Loughrey MB, Fernández JA, Dombrowski Y, McArt DG, Dunne PD, et al. QuPath: Open source software for digital pathology image analysis. *Sci Reports 2017 71* 2017;7:1–7.

[37] Ran D, Moharil J, Lu J, Gustafson H, Culm-Merdek K, Strand-Tibbitts K, et al. Platform comparison of HTG EdgeSeq and RNA-Seq for gene expression profiling of tumor tissue specimens. *Https://DoiOrg/101200/JCO20203815_suppl3566* 2020;38:3566–3566.

[38] Anders S, Huber W. Differential expression analysis for sequence count data. *Genome Biol* 2010;11.

[39] Benjaminit Y, Hochberg Y. Controlling the False Discovery Rate: a Practical and Powerful Approach to Multiple Testing. *J R Stat Soc B* 1995;57:289–300.

[40] Yu G, Wang LG, Han Y, He QY. ClusterProfiler: An R package for comparing biological themes among gene clusters. *Omi A J Integr Biol* 2012;16:284–7.

[41] Subramanian A, Tamayo P, Mootha VK, Mukherjee S, Ebert BL, Gillette MA, et al. Gene set enrichment analysis: A knowledge-based approach for interpreting genome-wide expression profiles. *Proc Natl Acad Sci U S A* 2005;102:15545–50.

[42] Akoglu H. User's guide to correlation coefficients. *Turkish J Emerg Med* 2018;18:91.

[43] Mukaka M. A guide to appropriate use of Correlation coefficient in medical research. *Malawi Med J* 2012;24:69.

[44] Schober P, Schwarte LA. Correlation coefficients: Appropriate use and interpretation. *Anesth Analg* 2018;126:1763–8.

[45] Verhoef EI, Kweldam CF, Kümmerlin IP, Nieboer D, Bangma CH, Incrocci L, et al. Characteristics and outcome of prostate cancer patients with overall biopsy Gleason score 3 + 4 = 7 and highest Gleason score 3 + 4 = 7 or > 3 + 4 = 7. *Histopathology* 2018;72:760–5.

[46] Schröder FH, Hugosson J, Roobol MJ, Tammela TLJ, Ciatto S, Nelen V, et al. Screening and Prostate-Cancer Mortality in a Randomized European Study. *Http://DxDoiOrg/101056/NEJMoa0810084* 2009;360:1320–8.

[47] Ahmed HU, El-Shater Bosaily A, Brown LC, Gabe R, Kaplan R, Parmar MK, et al. Diagnostic accuracy of multi-parametric MRI and TRUS biopsy in prostate cancer (PROMIS): a paired validating confirmatory study. *Lancet* 2017;389:815–22.

[48] Ståhl PL, Salmén F, Vickovic S, Lundmark A, Navarro JF, Magnusson J, et al. Visualization and analysis of gene expression in tissue sections by spatial

transcriptomics. *Science* 2016;353:78–82.

[49] Erickson A, He M, Berglund E, Marklund M, Mirzazadeh R, Schultz N, et al. Spatially resolved clonal copy number alterations in benign and malignant tissue. *Nat 2022 6087922* 2022;608:360–7.

[50] Owen KL, Gearing LJ, Zanker DJ, Brockwell NK, Khoo WH, Roden DL, et al. Prostate cancer cell-intrinsic interferon signaling regulates dormancy and metastatic outgrowth in bone. *EMBO Rep* 2020;21.

[51] Emerson L, Morales A. Intralesional recombinant α-interferon for localized prostate cancer: a pilot study with follow-up of >10 years. *BJU Int* 2009;104:1068–70.

[52] Xia Y, Shen S, Verma IM. NF-κB, an active player in human cancers. *Cancer Immunol Res* 2014;2:823.

[53] Witte KE, Pfitzenmaier J, Storm J, Lütkemeyer M, Wimmer C, Schulten W, et al. Analysis of several pathways for efficient killing of prostate cancer stem cells: A central role of nf-κb rela. *Int J Mol Sci* 2021;22.

[54] Torrealba N, Vera R, Fraile B, Martínez-Onsurbe P, Paniagua R, Royuela M. TGF-β/PI3K/AKT/mTOR/NF-kB pathway. Clinicopathological features in prostate cancer. *Aging Male* 2020;23:801–11.

[55] Hurlbut GD, Kankel MW, Lake RJ, Artavanis-Tsakonas S. Crossing paths with Notch in the hyper-network. *Curr Opin Cell Biol* 2007;19:166–75.

[56] Bin Hafeez B, Adhami VM, Asim M, Siddiqui IA, Bhat KM, Zhong W, et al. Targeted Knockdown of Notch1 Inhibits Invasion of Human Prostate Cancer Cells Concomitant with Inhibition of Matrix Metalloproteinase-9 and Urokinase Plasminogen Activator 2009.

[57] Ross AE, Marchionni L, Vuica-Ross M, Cheadle C, Fan J, Berman DM, et al. Gene Expression Pathways of High Grade Localized Prostate Cancer. *Prostate* 2011;71:1568–78.

[58] Hudson RS, Yi M, Esposito D, Watkins SK, Hurwitz AA, Yfantis HG, et al. MicroRNA-1 is a candidate tumor suppressor and prognostic marker in human prostate cancer. *Nucleic Acids Res* 2012;40:3689.

[59] Carvalho FLF, Simons BW, Eberhart CG, Berman DM. Notch Signaling in Prostate Cancer: A Moving Target. *Prostate* 2014;74:933.

[60] Vilchez Mercedes SA, Bocci F, Levine H, Onuchic JN, Jolly MK, Wong PK. Decoding leader cells in collective cancer invasion. *Nat Rev Cancer 2021 219* 2021;21:592–604.

[61] Wang L, Zi H, Luo Y, Liu T, Zheng H, Xie C, et al. Inhibition of Notch pathway

enhances the anti-tumor effect of docetaxel in prostate cancer stem-like cells. *Stem Cell Res Ther 2020 111* 2020;11:1–8.

[62] Cui J, Wang Y, Dong B, Qin L, Wang C, Zhou P, et al. Pharmacological inhibition of the Notch pathway enhances the efficacy of androgen deprivation therapy for prostate cancer. *Int J Cancer* 2018;143:645–56.

[63] Farah E, Li C, Cheng L, Kong Y, Lanman NA, Pascuzzi P, et al. NOTCH signaling is activated in and contributes to resistance in enzalutamide-resistant prostate cancer cells. *J Biol Chem* 2019;294:8543–54.

AUTEUR(E) : Nom : CHEN **Prénom : Kelly**

Date de soutenance : 19 septembre 2022

Titre de la thèse : Les modifications transcriptomiques corrélées à l'augmentation du pourcentage de Gleason 4 dans une cohorte de diagnostic du cancer de la prostate

Thèse - Médecine - Lille 2022

Cadre de classement : *Urologie*

DES + FST/option : *UROLOGIE*

Mots-clés : biomarqueurs, cancer de prostate, diagnostic, cancer, prostate, Gleason 4, pourcentage de Gleason 4, ARN, gènes

Résumé :
Introduction : Il est recommandé de rapporter le pourcentage de Gleason 4 (%G4) pour un adénocarcinome de la prostate de score de Gleason 7. L'objectif de cette étude était d'identifier les gènes dont l'expression varie avec le %G4 et les voies métaboliques sous-jacentes impliquées dans son émergence.
Méthodes : Les patients ont été sélectionnés dans l'étude INNOVATE, une cohorte britannique monocentrique de biopsies prostatiques ciblées par imagerie par résonnance magnétique. 51 biopsies contenant du Gleason 3 et/ou 4 sans Gleason 5 ont été incluses. Les zones tumorales ont été macrodisséquées pour analyse moléculaire. Les données d'expression génique de 2549 gènes associés au cancer ont été générées avec le système HTG EdgeSeq couplé à la plateforme Illumina Next Generation Sequencing. L'analyse de l'expression différentielle a été effectuée sur les extrêmes de la cohorte. Les gènes exprimés de manière différentielle ont été en outre étudiés sur l'ensemble de la cohorte dans une analyse corrélant leur expression avec le%G4 en tant que variable continue. Une analyse d'enrichissement a recherché les voies métaboliques surreprésentées à partir des ensembles de gènes Hallmark et Reactome.
Résultats : Nous avons identifié 15 gènes d'intérêt exprimés différentiellement entre un %G4 faible (0-10 %) et élevé (40-100 %), avec une valeur de p ajustée < 0,05. 12 gènes étaient régulés positivement (SPINK1, COMP, ADAMTS1, EFNB2, ISG15, CENPN, IRS2, JAG1, F2R, HEYL, EGR1 et ENG), tandis que 3 l'étaient négativement (CXCL13, BMP5 et ADRA1D). Lorsque ce panel a été testé pour sa corrélation linéaire avec le %G4 ajusté sur la proportion de cellules épithéliales dans l'échantillon, 5 d'entre eux étaient corrélés au %G4 avec un coefficient de corrélation de Pearson entre 0,41 et 0,56 (valeur p ajustée < 0,05). Les voies les plus pertinentes identifiées par l'analyse de la surreprésentation comprenaient la signalisation androgénique, la transduction du signal et la réponse immunitaire (NOTCH, interféron, TNFα) ainsi que les réponses cellulaires au stress.
Conclusion : Cette étude pilote sur %G4 a pu identifier des voies pertinentes avec la littérature existante, soutenant l'intérêt croissant pour l'interprétation du %G4 comme une variable continue plutôt que la séparation binaire de la maladie de score de Gleason 7 en 3+4 et 4+3 pour l'évaluation de l'agressivité du cancer de la prostate.

<u>Composition du Jury</u> :

Président : Monsieur le Professeur Arnauld VILLERS
Assesseurs : Monsieur le Professeur Xavier LEROY
Madame le Docteur Martine DUTERQUE-COQUILLAUD
Directeur de thèse : Monsieur le Docteur Jonathan OLIVIER